

Astronomy Constraints on Short-Distance Modifications to General Relativity from Spinning Binary Systems

Aline Nascimento Lins

*Departamento de Física Teórica e Experimental,
Universidade Federal do Rio Grande do Norte, Natal-RN 59078-970, Brazil*

Riccardo Sturani

*International Institute of Physics, Universidade Federal do Rio Grande do Norte,
Campus Universitário, Lagoa Nova, Natal-RN 59078-970, Brazil^{*}*

We investigate the possibility of testing short distance modifications to General Relativity via higher curvature terms in the fundamental gravity Lagrangian by analysing their impact on observations of spinning astronomical binary systems. By using effective field theory methods applied to the 2-body problem, generic lower bounds on the short-distance scale accompanying high curvature terms can be set. In particular we focus our analysis on the observation of spin-dependent effects in gravitational wave detections from compact binary coalescences and spin precession measure in double binary pulsars.

Keywords: General Relativity, High-order operators, Effective field theory, Binary systems

I. INTRODUCTION

The recent Gravitational Wave (GW) detections [1, 2] by the LIGO [3] and Virgo [4] large interferometers have opened a new chapter in the history of physics and astronomy, with countless new investigation which are now made possible. The output of GW detectors is processed via *matched-filtering* [5], which is particularly sensitive to the phase of the GW signals, bearing the imprint of both the astrophysical parameter of the source, like masses and spins, and of the details of the gravitational theory, well in its non-linear regime, ruling the motion of the 2-body system sourcing GWs.

^{*}Electronic address: alinelins@fisica.ufrn.br, riccardo@iip.ufrn.br

In the present work we admit the possibility that General Relativity (GR) may not be the ultimate theory of gravity but may be completed at *short distances* (UV henceforth) by higher curvature terms. We adopt the framework introduced by [6], i.e. we add *quartic* curvature terms of the type Riemann to the fourth power to the (gauge-fixed) Einstein-Hilbert Lagrangian and compute their lowest order effects, in both the spinning and non-spinning case, to the 2-body dynamics by using the effective field theory methods for gravity pioneered in [7], later applied also to spinning sources [8, 9], also known as Non-Relativistic GR (NRGR).

The introduction of higher curvature terms than in GR introduces new phenomenological constants (with dimensions) parametrising the strength of the GR modifications, playing the role of the UV cutoff of the effective theory.

We consider in this work astronomical observations of *spinning* binary systems, focusing on both detection of GWs from compact binary coalescences and observation of double binary pulsars, which also allow a measure of individual pulsar spin precession, the latter analysis extending the work of [6].

The paper is organised as follows: in sec. II we summarise the parametrisation of GR UV completion introduced in [6] and recall briefly the effective field theory method description of gravity for non-relativistic (i.e for small velocity) spinning systems [9, 10]. In sec. III we present the computation of the effects that higher-curvature terms have for both spinning and non spinning binaries on the energy and luminosity function which determine the GW-phasing, and on the spin precession in binary systems. A discussion of the results and comparisons with current observational limits are presented in sec. IV.

II. METHOD

Considering a generic parametrisation of possible UV completions of GR, we adopt the effective Lagrangian proposed in [6]

$$\mathcal{S}_{eff} = \frac{1}{16\pi G_N} \int d^4x \sqrt{-g} \left(R - \frac{1}{2}\Gamma^\mu\Gamma_\mu + \frac{\mathcal{C}^2}{\Lambda^6} + \frac{\mathcal{C}\tilde{\mathcal{C}}}{\Lambda_-^6} + \frac{\tilde{\mathcal{C}}^2}{\tilde{\Lambda}^6} \right), \quad (1)$$

with $\Gamma^\mu \equiv g^{\nu\rho}\Gamma^\mu_{\nu\rho}$ enters the gauge fixing term and

$$\begin{aligned} \mathcal{C} &\equiv R_{\alpha\beta\gamma\delta}R^{\alpha\beta\gamma\delta}, \\ \tilde{\mathcal{C}} &\equiv R_{\alpha\beta\gamma\delta}\epsilon^{\alpha\beta}_{\mu\nu}R^{\mu\nu\gamma\delta}. \end{aligned} \quad (2)$$

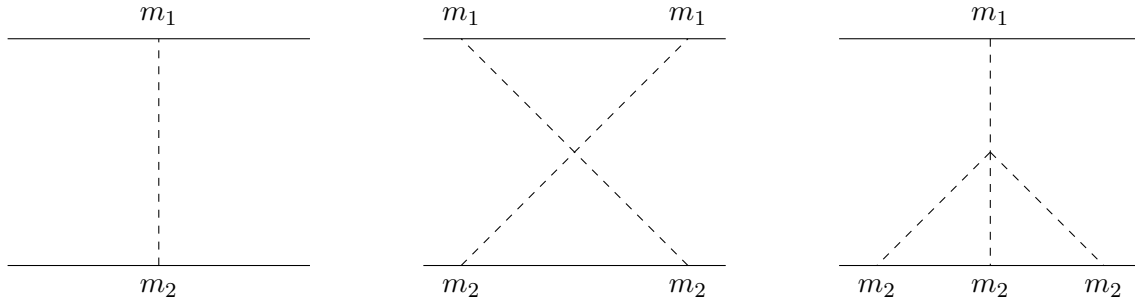


Figure 1: Feynman diagrams representing the Newtonian potential (first on the left) and the leading corrections from the Riemann⁴ terms in the fundamental Lagrangian in eq. (1). Last diagram must be supplemented with its mirror image under $m_1 \leftrightarrow m_2$.

Eq.(1) adds to the Einstein-Hilbert Lagrangian terms at *fourth* order of the curvature, where $\Lambda, \Lambda_-, \tilde{\Lambda}$ are constant with unit of inverse length. Terms quadratic in curvature tensors do not contribute to the equations of motions as they can be written in terms of total derivatives plus terms vanishing on the equations of motion, and cubic terms are forbidden by the causality argument presented in [11].

For non- or mildly-relativistic binary systems it is natural to expand perturbatively the dynamics according to the post-Newtonian (PN) approximation of GR, i.e terms at n -th PN order are of the type $G_N^{n-j+1}v^{2j}$, with $0 \geq j \geq n$, $n = j = 0$ corresponding to the leading order (LO) Newtonian potential, being v relative velocity of binary components.

The extra terms introduce bulk interactions of quartic and higher orders affecting the equation of motions and the radiation emission (note that to derive the GW phase dynamical evolution one needs both the energy of bound orbits and the luminosity function) for both non-spinning and spinning sources.

Defining $M \equiv m_1 + m_2$ the sum of rest masses of binary constituents $m_{1,2}$, and introducing for later use the reduced mass $\mu \equiv m_1 m_2 / M$ and the symmetric mass ratio $\eta \equiv \mu / M$, straightforward dimensional argument shows that the quartic interactions introduced above add to the two-body potential terms of the order of $(GM/r)^2 / (\Lambda r)^6$, leading to corrections of the order $2\text{PN} \times 1 / (\Lambda r)^6$, and analogously for the spin equations of motion, with exception for the parity violating term $\mathcal{C}\tilde{\mathcal{C}}$ that will be discussed later.

To make contact with the v expansion of the PN approximation, we find convenient to

express the metric via the Kaluza-Klein (KK) parametrisation [12]

$$g_{\mu\nu} = e^{2\phi/m_{Pl}} \begin{pmatrix} -1 & \frac{A_i}{m_{Pl}} \\ \frac{A_j}{m_{Pl}} & e^{-c_d\phi/m_{Pl}} \left(\delta_{ij} + \frac{\sigma_{ij}}{m_{Pl}} \right) - \frac{A_i A_j}{m_{Pl}^2} \end{pmatrix}, \quad (3)$$

with $m_{Pl} \equiv (32\pi G_N)^{-1/2}$, $c_d \equiv 2(d-1)/(d-2)$, where d is the number of space dimension, $d = 3$ in the rest of this work, and Latin indices i, j, \dots run over pure space dimensions. The quadratic terms of the gravity bulk Lagrangian, unaffected by the $\mathcal{C}^2, \mathcal{C}\tilde{\mathcal{C}}, \tilde{\mathcal{C}}^2$ terms, are then given by

$$\mathcal{S}_{eff} = \int d^{d+1}x \sqrt{-\gamma} \left\{ \frac{1}{4} [(\nabla_k \sigma)^2 - 2(\nabla_k \sigma_{ij})^2 - (\dot{\sigma}^2 - 2(\dot{\sigma}_{ij})^2)] - c_d [(\nabla_k \phi)^2 - \dot{\phi}^2] + \left[\frac{1}{2} F_{ij}^2 + (\nabla_k A_i)^2 - \dot{A}_i^2 \right] \right\}, \quad (4)$$

with $\sigma \equiv \sigma_{ij} \delta^{ij}$, where time and space-derivatives have been split to make manifest the scaling in v of the potential modes as their derivatives scale differently with v : $\frac{d}{dt} \sim v^i \partial_i$.

The parametrisation in eq. (3) has the advantage that expanding around the Minkowski metric $\eta_{\mu\nu} \equiv \text{diag}(-1, 1, 1, 1)$ it returns diagonal Feynman propagators for the fields ϕ, A_i, σ_{ij} [13, 14]:

$$\left. \begin{aligned} P[\phi, \phi] &= -\frac{1}{8} \\ P[A_i, A_j] &= \frac{\delta_{ij}}{2} \\ P[\sigma_{ij}, \sigma_{kl}] &= -\frac{1}{2} (\delta_{ik} \delta_{jl} + \delta_{il} \delta_{jk} - 2\delta_{ij} \delta_{kl}) \end{aligned} \right\} \times \frac{i}{\vec{k}^2 - k_0^2 - i\epsilon}. \quad (5)$$

A. Spin-less case

1. Two-body potential in GR

The standard coupling to gravity of a spin-less particle of mass m_a with trajectory x_a is given by the world-line

$$\mathcal{S}_{pp-wl}|_{\vec{S}=0} = -m_a \int dx_a \tau \supset \frac{m_a}{m_{Pl}} \int_{x_a} dt \left[-\phi + A_i v_i + \frac{1}{2} \sigma_{ij} v^i v^j + \dots \right], \quad (6)$$

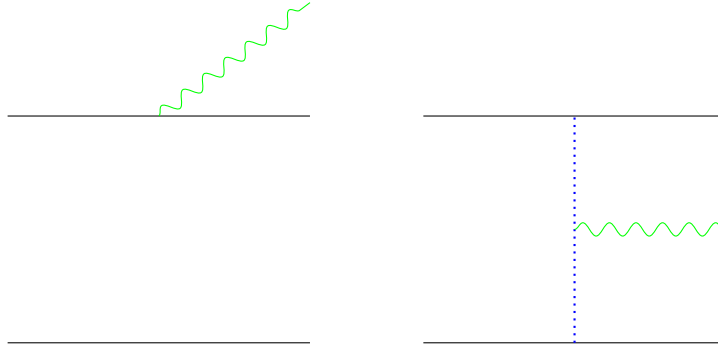


Figure 2: Diagrams describing LO radiative process from a spin-less binary system. The first one must be supplemented by its mirror image under $1 \leftrightarrow 2$. Green wavy lines represent radiation, blue dotted line are ϕ longitudinal modes.

where dots stand for non-linear coupling with gravity fields and higher order in velocity expansion. The lowest order potential is given by the first diagram in fig. 1¹

$$V_N = -\frac{m_1 m_2}{8m_{Pl}^2} \int_{\mathbf{k}} \frac{e^{i\vec{k}\cdot\vec{r}}}{k^2} = -\frac{G_N m_1 m_2}{r}, \quad (7)$$

which is the standard Newton potential, obtained by taking the static limit of both the world-line action eq. (6) and of the propagators (5). The additional diagrams in fig. 1 are the LO diagrams modifying the Newtonian potential due to Riemann⁴ terms in eq. (1).

2. Radiation emission in GR

The coupling of a binary system to radiative gravitational modes in GR can be computed via the diagrams in fig. 2 [7], i.e. by analysing the emission of a (trace-less) σ_{ij} mode, which gives the following LO effective Lagrangian:

$$\mathcal{L}_{rad-I} = \frac{1}{2} T^{ij} \frac{\sigma_{ij}}{m_{Pl}} \quad (8)$$

$$= m_1 \left(v_1^i v_1^j - \frac{G_N m_2 r^i r^j}{2r^3} \right) \frac{\sigma_{ij}}{m_{Pl}} + (1 \leftrightarrow 2). \quad (9)$$

By using the (spin-less) Newtonian equation of motion

$$\vec{a}_1|_{\vec{S}_{1,2}=0} = -\frac{G_N m_2 \vec{r}}{r^3}, \quad (10)$$

¹ We adopt the notation $\int_{\mathbf{k}} \equiv \int \frac{d^d k}{(2\pi)^d}$ and $d = 3$ throughout this paper.

one can recast eq. (9) into the following standard form

$$\mathcal{L}_{rad-I} = \frac{1}{2} I^{ij} R_{0i0j} , \quad (11)$$

where I^{ij} is the radiative electric quadrupole which at LO equals the (trace-less) mass quadrupole $Q^{ij} = \sum_{a=1}^2 m_a (x_a^i x_a^j - \frac{1}{3} \delta^{ij} x_a^2)$ and R_{0i0j} is the *electric* part of the Riemann tensor, whose explicit expression at linear order in the metric perturbation reads:

$$m_{Pl} R_{0i0j} \simeq \frac{1}{2} \left(\ddot{\sigma}_{ij} - \dot{A}_{i,j} - \dot{A}_{j,i} \right) - \phi_{,ij} - \frac{\delta_{ij}}{d-2} \ddot{\phi} . \quad (12)$$

More generally, the radiative coupling can be equivalently expressed either in terms of moments of space-space components the energy-momentum tensor like in (8), or in terms of mass and momentum multipole moments like in (11). The derivation of the equivalence is a standard GR-course exercise which uses the conservation of the energy-momentum tensor

$$T^{\mu\nu}_{,\nu} = 0 , \quad (13)$$

and we report here the radiative multipolar coupling up to NLO in terms of the electric octupole O^{ijk} and the magnetic quadrupole J^{ij} , see app. A for details,

$$\mathcal{L}_{rad-GR} = \int dt \left(\frac{1}{2} I^{ij} \mathcal{E}_{ij} + \frac{1}{6} O^{ijk} \mathcal{E}_{ij,k} + \frac{2}{3} J^{ij} \mathcal{B}_{ij} \right) + \text{higher multipoles} , \quad (14)$$

where $\mathcal{E}_{ij} = R_{0i0j}$ and $\mathcal{B}_{ij} = \frac{1}{2} \epsilon_{ikl} R_{0jkl}$ is the magnetic part of the Riemann tensor. Note that since \mathcal{E}_{ij} and \mathcal{B}_{ij} are trace-less, as the radiative multipoles. From (14) one can derive the standard GR flux formula which is given, writing explicitly only the electric and magnetic quadrupole contributions, by [15]

$$F = G_N \left(\frac{1}{5} \ddot{I}_{ij}^2 + \frac{16}{45} \ddot{J}_{ij}^2 + \dots \right) , \quad (15)$$

from which the electric quadrupole contribution gives the LO formula for emission of GWs from circular orbits $F_{LOcirc} = \frac{32}{5G_N} \eta^2 v^{10}$.

B. Spin degrees of freedom in GR

Spin degrees of freedom in GR require the introduction of additional degrees of freedom than just position and velocity, embodied by two tetrads: e_a^μ , relating the metric into the locally free-falling frame [16, 17]

$$g_{\mu\nu} e_a^\mu e_b^\nu = \eta_{ab} , \quad (16)$$

and e_A^μ , co-rotating with the spinning body, and related to the former by a local Lorentz transformation $e_A^\mu = \Lambda_A^a e_a^\mu$ (we use a, b, c, d to denote flat space-time Lorentz indices with their capitalised version transforming under the residual Lorentz invariance).

The transport of e_A^μ along the world-line of a reference point chosen inside the extended body defines the generalised angular velocity $\Omega^{\mu\nu}$

$$\frac{de^{A\mu}}{d\tau} \equiv u^\rho e_{;\rho}^{A\mu} = \Omega_\nu^\mu e^{A\nu} \implies \Omega^{\mu\nu} = e_A^\mu \frac{de^{A\nu}}{d\tau} = -\Omega^{\nu\mu}, \quad (17)$$

where u^ρ is the four-velocity of the object's world-line. Local coordinate, Lorentz and parametrisation invariances require the Lagrangian to be made of invariant contractions of $\Omega^{\mu\nu}$, u^ρ and eventually of the local curvature tensors, but do not unambiguously fix its form even in the case of flat space-time. However it turns out that if one neglects finite-size effects the variation of any possible Lagrangians w.r.t. to the spinning body local position and tetrad, when expressed in terms of the conjugate momenta $p^\mu = \frac{\delta\mathcal{L}}{\delta u_\mu}$ and $S^{\mu\nu} = \frac{\delta\mathcal{L}}{\delta\Omega_{\mu\nu}}$, gives the *Mathisson-Papapetrou* equations of motion [18–20]:

$$\begin{aligned} \frac{dp^\mu}{d\tau} &= -\frac{1}{2} R_{\mu\nu\rho\sigma} u^\nu S^{\rho\sigma}, \\ \frac{dS^{\mu\nu}}{d\tau} &= p^\mu u^\nu - p^\nu u^\mu. \end{aligned} \quad (18)$$

Since the physical spin variables are related to the conjugate momentum $S^{\mu\nu}$ rather than to the fundamental tetrad variables, it can be convenient to work with a functional that behaves as an Hamiltonian with respect to the spin, while remaining a Lagrangian with respect to the body position x^μ . Such hybrid functional is called a Routhian [21], defined as the Legendre transform of the Lagrangian \mathcal{L} , which gives the explicit form (valid up to linear order in the spin)

$$\mathcal{R} = m\sqrt{u^2} + \frac{1}{2} \omega_\mu^{ab} S_{ab} u^\mu, \quad (19)$$

being $\omega_\mu^{ab} \equiv e^{b\nu} e_{\nu;\mu}^a$ the spin connection. One then recovers the Mathisson-Papapetrou equations via

$$\frac{\delta}{\delta x^\mu} \int dt \mathcal{R} = 0, \quad \frac{dS^{ab}}{d\tau} = \{\mathcal{R}, S^{ab}\}, \quad (20)$$

once the following Poisson bracket is taken into account²:

$$\{S^{ab}, S^{cd}\} = \eta^{ad}S^{bc} + \eta^{bc}S^{ad} - \eta^{ac}S^{bd} - \eta^{bd}S^{ac}. \quad (21)$$

The anti-symmetric tensor $S^{\mu\nu}$ (which appears above through its locally flat-frame components $S^{ab} \equiv S^{\mu\nu}e_\mu^a e_\nu^b$) is the generalised, relativistically-covariant spin of the body, however it contains redundant degrees of freedom. The redundancy corresponds to the ambiguity related the choice of a reference world-line inside the body. One can reduce from 6 to the 3 degrees of freedom needed to describe an ordinary spin vector by imposing the *Spin Supplementary Condition* (SSC), which relates the 3-vector S^{0i} to the physical spin components $S^i \equiv \frac{1}{2}\varepsilon^{ijk}S_{jk}$. There is not a unique way to impose such condition, e.g. one can use the *covariant* SSC $S^{\mu\nu}p_\nu = 0$ condition [16], the *baryonic* $S^{i0} = \frac{1}{2}S^{ij}u_j$ [22], among others, both of which can be described at LO by

$$S^{i0} = \kappa S^{ij}v_j, \quad (22)$$

with $\kappa = 1, \frac{1}{2}$. The requirement of SSC conservation along the world line shifts the momentum of the particle by a quantity *quadratic* in the spin [16], and it will be neglected in this work that is restricted to liner-in-spin effects.

Being an algebraic constraint, as far as the orbital equation of motions are concerned, the SSC can be imposed by direct replacement of S^{i0} indifferently at the level of the fundamental Routhian, in the effective potential or in the equations of motion: we will adopt here the second option (substitute into the potential). However when deriving the spin equations of motion the SSC constraint has to be imposed at the level of the equation of motions, i.e. after applying the Poisson bracket in eq. (20).

Note that adopting the covariant SSC, i.e. $\kappa = 1$ in eq. (22), the Poisson brackets become *non-canonical*: brackets between coordinates and between coordinates and spin do not vanish [16]. Instead of dealing with a non-canonical algebra one can equivalently shift the world-line of each particle according to [17]

$$\vec{x}_{1,2} \rightarrow \vec{x}_{1,2} - \frac{1}{2m_{1,2}}\vec{S}_{1,2} \times \vec{v}_{1,2}, \quad (23)$$

² Note the difference in sign with respect to eq. (8.25) of [9], where a mostly minus metric signature convention is used.

and use a canonical algebra when deriving the equation of motions for coordinates and spin, or equivalently one can adopt the baryonic SSC, $\kappa = 1/2$ in eq. (22), and use canonical Poisson brackets [17].

The spin-dependent part of the world-line action in terms of the KK parametrisation, for a particle with mass m and velocity v at linear order in spin is (for $d = 3$)³ [23]

$$\mathcal{S}_{pp-wl} \supset \frac{1}{m_{Pl}} \int_{x_a} dt \left[S^{ij} \left(-\frac{1}{4} F_{ij} + \frac{1}{2} \sigma_{ik,j} v_a^k + \phi_{,j} v_{ai} + \frac{1}{4} F_{jk} \sigma_i^k + \frac{1}{2} \sigma_{ik} (\phi_{,j} v_a^k + \phi^{,k} v_{aj}) \right) + S^{0i} \left(-\phi_{,i} + \frac{1}{2} \dot{\sigma}_{ij} v_a^j - \frac{1}{2} \phi_{,j} \sigma_{ij} \right) \right], \quad (24)$$

where all field are understood to be evaluated on the world-line of the source-particle and we displayed only terms that will be needed in the rest of this work.

For power counting spin $|\vec{S}_a| \sim G_N m_a^2$, angular momentum $|\vec{L}| \sim \eta G_N M^2/v$ hence terms linear in spin, i.e. of the type $\vec{S} \times L$ appear earlier than terms $\sim \vec{S}^2$ in the PN expansion.

1. Spin terms in two-body potential in GR

The lowest order spin contribution to the body potential in GR occurs at 1.5PN order, i.e. v^3 order with respect to the leading, and is due to the sum of the two processes represented in fig. 3 (and their mirror images under $1 \leftrightarrow 2$).

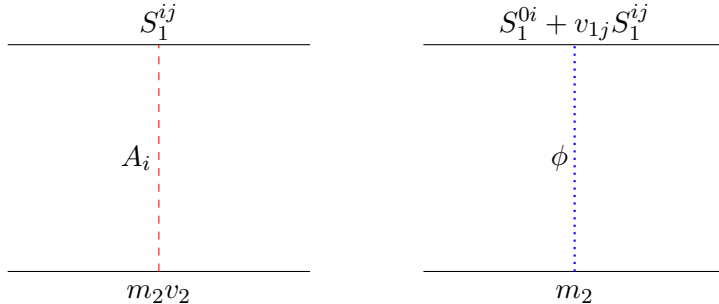


Figure 3: Diagrams representing the LO spin-orbit potential in GR. Diagrams must be supplemented with their $1 \leftrightarrow 2$ mirror image. Dashed red line represent a A_i -polarised longitudinal mode, blue dotted lines are ϕ -modes.

³ Note that the point-particle Routhian has the same sign as the potential, hence opposite sign with respect to the Lagrangian.

The sum of the exchange of gravitational modes with A_i and ϕ polarisations reported in fig. 3, with vertices given by the Lagrangian (24) gives ($\vec{r} \equiv \vec{x}_1 - \vec{x}_2$) for the LO spin-dependent (*spin-orbit*) potential

$$V_{SO}^{(LO)} = 2 \frac{G_N m_2}{r^3} \vec{S}_1 \cdot (\vec{r} \times \vec{v}) + (\kappa - 1) \frac{G_N m_2}{r^3} \vec{S}_1 \cdot (\vec{r} \times \vec{v}_1) + 1 \leftrightarrow 2. \quad (25)$$

After substituting the covariant SSC (22) with $\kappa = 1$ one obtains a different result than the classical one [22, 24, 25] which implicitly uses $\kappa = 1/2$, however things reconcile at the level of the equation of motions. Indeed using the covariant SSC (i.e. $\kappa = 1$), the spin equations of motion, which are first order, are obtained by using the second of the eqs. (20), *then* applying the SSC, giving:

$$\dot{S}_1^i = \frac{1}{2} \epsilon^{ijk} \left\{ V_{SO}^{(L)}, S_{1jk} \right\} = \frac{G_N m_2}{r^2} \left[\vec{S}_1 \times (\hat{n} \times (2\vec{v}_2 - \vec{v}_1)) + \hat{n} \times (\vec{v}_1 \times \vec{S}_1) \right]^i, \quad (26)$$

which implies that the norm of \vec{S}_1 is not conserved, since $\dot{\vec{S}}_1$ is not perpendicular to \vec{S}_1 . The previous result can be recast into the standard one by performing the $O(v^2)$ shift of the spin variable according to

$$\vec{S}_a \rightarrow \left(1 - \frac{v_a^2}{2} \right) \vec{S}_a + \frac{\vec{v}_a}{2} \left(\vec{v}_a \cdot \vec{S}_a \right), \quad (27)$$

for $a = 1, 2$. The shift (27) (together with the shift (23) to be used for $\kappa = 1$ only) recast the non-canonical Poisson brackets into canonical ones, finally obtaining a spin vector with constant norm (neglecting absorption effects [26]), and whose derivative at LO, after substituting the center of mass relationships

$$\vec{v}_1 = \frac{m_2}{M} \vec{v}, \quad \vec{v}_2 = -\frac{m_1}{M} \vec{v}, \quad (28)$$

is given by the standard form [27, 28]

$$\frac{d\vec{S}_1}{dt} = \frac{G_N}{r^3} \left[2 + \frac{3m_2}{2m_1} \right] \vec{L} \times \vec{S}_1, \quad (29)$$

being $\vec{L} \equiv \mu \vec{r} \times \vec{v}$ the Newtonian orbital angular momentum, with μ the reduced mass. The result in eq. (29) could have been obtained straightforwardly by substituting relations (28) and $\kappa = 1/2$ into the potential (25) and then applying canonical Poisson brackets, without the shifts (23) and (27) [22].

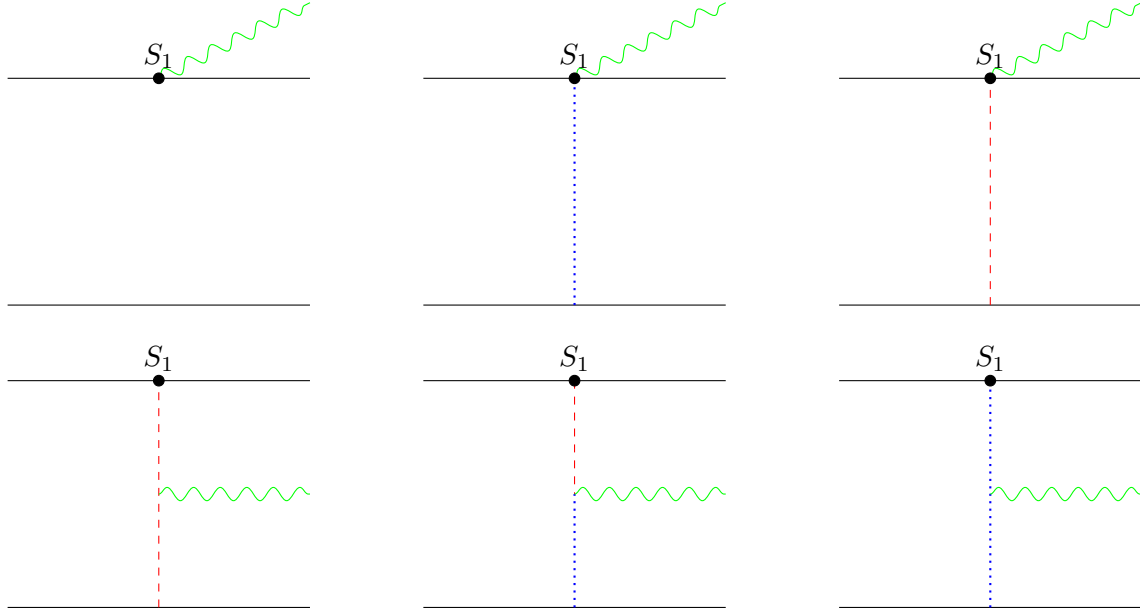


Figure 4: Diagrams determining (part of) the LO spin terms in gravitational radiation emission. The first one contributes at LO to the magnetic quadrupole, the remaining ones to the electric quadrupole. Additional contribution comes from the expression of the radiative multipoles in terms of the energy-momentum tensor, see app. A.

Eq. (29) is responsible for the precession of the spin around the orbital angular momentum⁴ with angular velocity $\Omega_S \sim v^3/r$, i.e. the precession time scale is longer than the orbital scale r/v but shorter than the typical dissipation time-scale $\eta^{-1}r/v^5$.

Finally, from the potential (25) and the world-line coordinate shift (23) one can derive the Newtonian equation of motion including effects linear in spin for the relative acceleration of two point-particles at LO in v [27]:

$$\vec{a} = -\frac{G_N M \vec{r}}{r^3} + 2 \frac{G_N}{r^3} \left[2 \left(\vec{S}_m \times \vec{v} \right) + 3 \frac{\vec{r} \cdot \vec{v}}{r^2} \left(\vec{r} \times \vec{S}_m \right) + 3 \frac{\vec{r}}{r^2} \left(\vec{S}_m \cdot (\vec{r} \times \vec{v}) \right) \right], \quad (30)$$

where $\vec{S}_m \equiv \left(1 + \frac{3m_2}{4m_1}\right) \vec{S}_1 + \left(1 + \frac{3m_1}{4m_2}\right) \vec{S}_2$. Also in this case the equation of motion (30) can be obtained straightforwardly from the potential (25) with $\kappa = 1/2$.

⁴ The orbital angular momentum is usually larger than individual spins, unless $\eta \ll 1$ and $v \lesssim 1$.

2. Spin terms in radiation emission in GR

The lowest order spin-dependent source coupling to σ_{ij} is given by the diagrams in fig. 4. The first diagram does not involve any field propagator, hence it can be directly read from the Lagrangian, and its leading contribution from the $\sim S^{ij}\sigma_{ik,j}v^j$ term in eq. (24) is of *magnetic* quadrupole type

$$\mathcal{L}_{rad-JS} = \frac{1}{2}S_{1ij}\frac{\sigma_{jk,i}}{m_{Pl}}v_1^k + 1 \leftrightarrow 2 = \frac{1}{4}(S_1^i x_1^j + S_1^j x_1^i + 1 \leftrightarrow 2)\frac{\epsilon^{ikl}}{2m_{Pl}}(\dot{\sigma}_{ik,l} - \dot{\sigma}_{il,k}) , \quad (31)$$

implying by comparison with eq. (14) that the spinning part of the magnetic quadrupole J^{ij} is

$$J_S^{ij} = \frac{3}{4}\sum_a(S_a^i x_a^j + S_a^j x_a^i)_{TF} , \quad (32)$$

where TF stands for trace-free part.

The first diagram in fig. 4 also includes the $S^{0i}\phi_{,j}\sigma_{ij}$ interaction from the Lagrangian (24) which contributes to the electric quadrupole coupling as

$$\begin{aligned} \mathcal{L}_{rad-QSI} &= \left[\frac{1}{2}\frac{d}{dt}(S_1^{i0}v_1^j + S_1^{j0}v_1^i) + 1 \leftrightarrow 2\right]\frac{\sigma_{ij}}{2m_{Pl}} \\ &= -\frac{\kappa G_N m_2^2}{2Mr^3}\left[\left(\vec{v} \times \vec{S}_1\right)^i r^j + \left(\vec{r} \times \vec{S}_1\right)^i v^j + i \leftrightarrow j\right]\frac{\sigma_{ij}}{2m_{Pl}} + 1 \leftrightarrow 2 , \end{aligned} \quad (33)$$

where in the second line the equation of motion (10) and the center of mass relationships (28) have been used.

The 5 remaining diagrams in fig. 4 contribute to the electric quadrupole, the leading contribution is of order v with respect to (31) giving in total:

$$\begin{aligned} \mathcal{L}_{rad-QSII} &= \frac{G_N m_2}{r^3}\left\{-\left[\left(\frac{\kappa+3}{2}\vec{v}_1 - 2\vec{v}_2\right) \times S_1\right]^i r^j - \frac{1}{2}\left(\vec{r} \times \vec{S}_1\right)^i v_1^j\right. \\ &\quad \left.+ 3r^i(\vec{r} \cdot \vec{v})\left(\vec{r} \times \vec{S}_1\right)^j + \frac{3}{2}r^i r^j\left[\left(\vec{r} \times ((1+\kappa)\vec{v}_1 - 2\vec{v}_2)\right) \cdot \vec{S}_1\right]\right\}\frac{\sigma_{ij}}{m_{Pl}} + 1 \leftrightarrow 2 \\ &= \frac{G_N m_2}{Mr^3}\left\{-\left(\frac{\kappa+3}{2}m_2 + 2m_1\right)(\vec{v} \times S_1)^i r^j - \frac{1}{2}\left(\vec{r} \times \vec{S}_1\right)^i v^j\right. \\ &\quad \left.+ 3Mr^i(\vec{r} \cdot \vec{v})\left(\vec{r} \times \vec{S}_1\right)^j + \frac{3}{2}r^i r^j((1+\kappa)m_2 + 2m_1)(\vec{r} \times \vec{v}) \cdot \vec{S}_1\right\}\frac{\sigma_{ij}}{m_{Pl}} + 1 \leftrightarrow 2 , \end{aligned} \quad (34)$$

where in the last passage the center of mass relationships (28) have been inserted.

Eqs.(33,34) gives the explicit form of the linear coupling of the sources to σ_{ij} , i.e. of T^{ij} , as per eq. (8). To check that this result coincides with the standard one eq. (11), one has

to use the conservation of the energy momentum tensor (equivalent to the source equations of motion) eq. (13) to reproduce the quadrupole moment from T_{ij} via the standard GR textbook trick reported in app. A.

Indeed the linear-in-spin mass quadrupole

$$Q_S^{ij} \equiv \int_V T^{00} \Big|_S x^i x^j = (S_1^{i0} x_1^j + S_1^{j0} x_1^i) + 1 \leftrightarrow 2, \quad (35)$$

satisfies $\ddot{Q}^{ij} = 2 \int_V T^{ij}$ on the equations of motion with T^{ij} obtained from $\mathcal{L}_{rad-QSI+II} = \frac{1}{2} T^{ij} \sigma_{ij} / m_{Pl}$, i.e. from the sum of eqs. (33) and (34), considering the contribution of the equation of motion (30) coming from the difference between (9) and (11), using $\kappa = 1/2$.⁵

In the spinning case however, the radiative quadrupole I^{ij} coupling to the Riemann as per eq. (11) does not coincide with the mass quadrupole even at LO, as it is rather given by [25]

$$\begin{aligned} I^{ij} &= \int_V \left(T^{00} + T^{ll} - \frac{4}{3} \dot{T}^{0l} x^l \right) (x^i x^j)_{TF} \\ &= \left\{ (\kappa + 1) \left[(\vec{v}_1 \times \vec{S}_1)^i r^j \right] - \frac{2}{3} \left[(\vec{v}_1 \times \vec{S}_1)^i \vec{r}_1^j + (\vec{r}_1 \times \vec{S}_1)^i \vec{v}_1^j \right] + i \leftrightarrow j \right\}_{TF} + 1 \leftrightarrow 2, \end{aligned} \quad (36)$$

where for T^{0l} , T^{ij} we inserted their LO expressions that can be read directly from the Lagrangian (6): $\frac{1}{4} S_a^{ij} F_{ji}$ and $\frac{1}{2} S_a^{ik} v_a^j \sigma_{ij,k}$.

Had not we used the GR equations of motions, we would have obtained the coupling

$$\mathcal{L}_{rad} = \frac{\sigma_{ij}}{2m_{Pl}} \int_V \left[T^{ij} + \frac{1}{7} \frac{d^2}{dt^2} \left(\frac{2}{3} T^{ll} x^i x^j + \frac{11}{6} T^{ij} r^2 - T^{il} x^l x^j - T^{jl} x^l x^i \right) \right]_{TF}, \quad (37)$$

which is equivalent to (11) in GR, see app. A for details and derivation.

In total one has the electric quadrupole coupling, for $\kappa = 1/2$ and in the center of mass:⁶

$$\mathcal{L}_{rad-IS} = -\frac{1}{6} \frac{G_N m_2^2}{Mr^3} \left[(\vec{r} \times \vec{S}_1)^i v^j + (\vec{v} \times \vec{S}_1)^i r^j - \frac{3}{2} \frac{(\vec{r} \cdot \vec{v})}{r^2} (\vec{S}_1 \times \vec{r})^i r^j \right] \frac{\sigma_{ij}}{m_{Pl}} + 1 \leftrightarrow 2 \quad (38)$$

III. RESULTS FOR RIEMANN⁴ TERMS

To systematically show the results when short-scale deviations from GR are present, we present separately the effects of the terms \mathcal{C}^2 , $\mathcal{C}\tilde{\mathcal{C}}$ and $\tilde{\mathcal{C}}^2$ of eq. (1).

⁵ We use here the baryonic SSC for simplicity, to avoid the complication of a non-standard Poisson algebra, see eq. (A2) for details.

⁶ Note that using the LO expression for the linear in spin T^{ij} the term $\frac{d^2}{dt^2} (T^{il} x^l x^j + T^{jl} x^l x^i)$ in eq. (37) vanishes.

A. \mathcal{C}^2

The Riemann to the fourth power addition to the GR Lagrangian introduce 4-point interactions that change both the potential and the emission formulae. The spin-less LO corrections depending on the \mathcal{C}^2 terms can be derived from the contributions of diagrams in fig. 5 for the potential, and fig. 7 for the emission, which gives G_N^2 (or equivalently v^4) corrections with respect to the LO energy and emitted radiation flux.

Considering effects linear in spin with the lowest number of velocity factors (i.e. the lowest PN order), one has to compute the four-point vertex involving the lowest number of time derivative and velocities (and neglecting terms vanishing on the equations of motion), hence one can approximate

$$\begin{aligned} \mathcal{C} \simeq \frac{8}{m_{Pl}^2} & \left\{ (\partial_i \partial_j \phi) (\partial^i \partial^j \phi) + \left(\partial_i \dot{A}_j (\partial^i \partial^j \phi) - (\partial_i \partial_j A^j) \partial_i \dot{\phi} \right) - \frac{1}{2} (\ddot{\sigma}_{ij} + \nabla^2 \sigma_{ij}) (\partial^i \partial^j \phi) \right. \\ & + (\partial_i \partial_j \phi) \partial^i \partial_k \left(\sigma^{jk} - \frac{\delta^{jk}}{2} \sigma \right) + \frac{1}{2} \partial_i (\partial_k A_j - \partial_j A_k) \partial_k \dot{\sigma}_{ij} \\ & \left. + \frac{1}{8} (\partial_i \partial_j \sigma_{kl}) [(\partial_i \partial_j \sigma_{kl}) + (\partial_k \partial_l \sigma_{ij}) - 2 (\partial_i \partial_k \sigma_{jl})] + \dots \right\}, \end{aligned} \quad (39)$$

$$\begin{aligned} \mathcal{C}^2 \simeq \frac{64}{m_{Pl}^4} & (\partial_m \partial_n \phi) (\partial^m \partial^n \phi) \times \left\{ (\partial_i \partial_j \phi) (\partial_i \partial_j \phi) + 2 \left[\partial_i \dot{A}_j (\partial^i \partial^j \phi) - (\partial_i \partial_j A^j) \partial_i \dot{\phi} \right] \right. \\ & - (\ddot{\sigma}_{ij} + \nabla^2 \sigma_{ij}) (\partial^i \partial^j \phi) + 2 (\partial_i \partial_j \phi) \partial^i \partial_k \left(\sigma^{jk} - \frac{\delta^{jk}}{2} \sigma \right) + \partial_i (\partial_k A_j - \partial_j A_k) \partial_k \dot{\sigma}_{ij} \\ & \left. + \frac{1}{4} (\partial_i \partial_j \sigma_{kl}) [(\partial_i \partial_j \sigma_{kl}) + (\partial_i \partial_j \sigma_{kl}) - 2 (\partial_i \partial_k \sigma_{jl})] + \dots \right\}. \end{aligned} \quad (40)$$

Note that the potential gravitational mode A_i couples to world-line spin without time derivative or power of velocity, whereas ϕ and σ_{ij} require one power of velocity or a time derivative, see eq. (24).

1. Potential

No spin

The lowest order spin-dependent contributions to the potential due to the \mathcal{C}^2 term are given by the processes represented in fig. 5, plus their mirror image under $1 \leftrightarrow 2$ exchange. They correspond to the the “cross” and “peace/log” diagrams as they were named in [6].

The LO contribution to the potential is ⁷, see app. B 1 a for details,

$$\Delta V_\Lambda = -V_N \frac{256}{(\Lambda r)^6} \left(\frac{G_N m_2}{r} \right)^2 + 1 \leftrightarrow 2, \quad (41)$$

where V_N is the standard Newtonian potential, modifying the spin-independent part of the equation of motion to

$$\vec{a}_\Lambda = \vec{a}_{1\Lambda} - \vec{a}_{2\Lambda} = -\frac{G_N M \vec{r}}{r^3} \left[1 - \frac{2304}{(\Lambda r)^6} \frac{G_N^2 (m_1^2 + m_2^2)}{r^2} \right]. \quad (42)$$

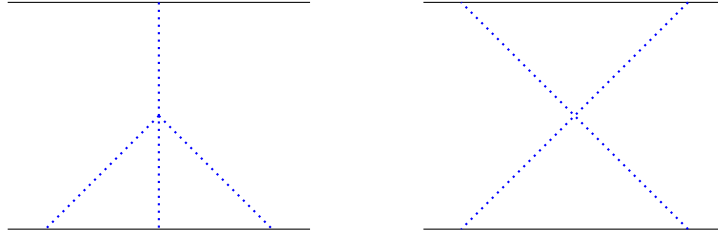


Figure 5: Diagrams representing the leading corrections to the non-spinning potential from \mathcal{C}^2 interactions (blue dotted lines represent ϕ propagators). The cross diagram vanishes. The diagram with one insertion in the upper line must be complemented by its mirror image under particle exchange.

Spin

The LO, linear-in-spin contribution to the potential can be derived by computing the diagrams in fig. 6, see app. B 2 a for details. They are all diagrams with 1 power of the spin and 1 power of the velocity of any of the two particles (there are no spin-dependent contributions for $\vec{v}_1 = \vec{v}_2 = 0$).

Overall they give the following potential

$$\Delta V_{\Lambda S_1} = -(1 + \kappa) \frac{2304}{(\Lambda r)^6} \vec{S}_1 \cdot (\vec{r} \times v_1) \frac{G_N^3 m_2 (m_1^2 + m_2^2)}{r^5} + (1 \leftrightarrow 2), \quad (43)$$

leading to a modification of the equation of motion

$$\Delta \vec{a}_{\Lambda S} = -3456 \frac{G_N^3 (1 - 2\eta) M^2}{\Lambda^6 r^{11}} \left[2 \left(\vec{S}_c \times \vec{v} \right) + 11 \frac{\vec{r} \cdot \vec{v}}{r^2} \left(\vec{r} \times \vec{S}_c \right) + 11 \frac{\vec{r}}{r^2} \left(\vec{S}_c \cdot (\vec{r} \times \vec{v}) \right) \right] \quad (44)$$

where $\eta \equiv m_1 m_2 / M^2$ and $\vec{S}_c \equiv \frac{1}{M} \left(\frac{m_2^2}{m_1} \vec{S}_1 + \frac{m_1^2}{m_2} \vec{S}_2 \right)$.

⁷ In [6] eq. (41) was computed for the first time, finding twice our result.

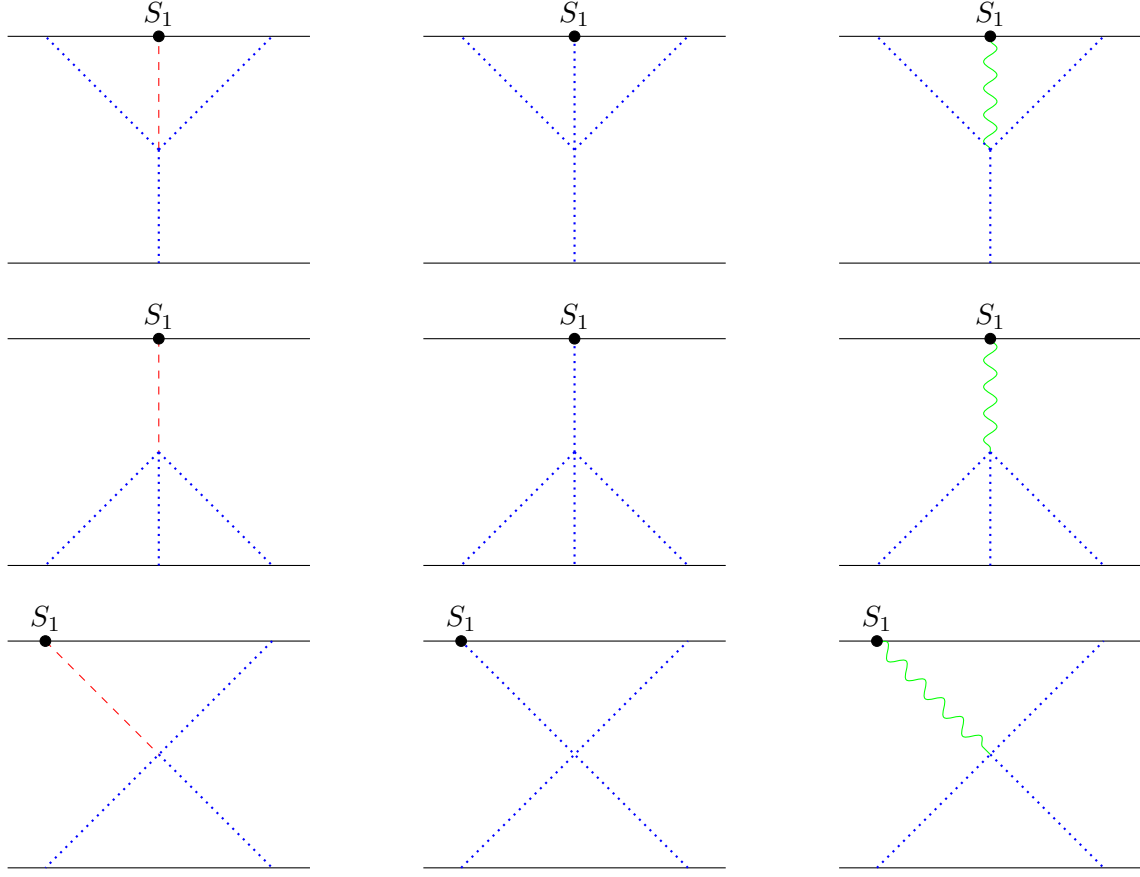


Figure 6: Diagrams representing the leading corrections to the linear-in-spin potential from \mathcal{C}^2 interactions. Blue dotted lines represent ϕ propagators, red dashed for A , green wavy for σ . All cross diagrams vanish, as well as the first (diagram with the field A coupling to S_1) and third (σ coupling to S_1) diagrams on the second line. Diagrams obtained by exchange particles 1 and 2 should be added.

The spin equation of motion with the contribution of the \mathcal{C}^2 interaction are obtained following the same procedure as the one used in sec. II to derive the LO spin-orbit coupling, to obtain the \mathcal{C}^2 correction

$$\Delta \left[\frac{d\vec{S}_1}{dt} \right]_{\Lambda} = -\frac{3456}{(\Lambda r)^6} \frac{G_N^3 (m_1^2 + m_2^2)}{r^5} \left(\frac{m_2}{m_1} \right) \vec{L} \times \vec{S}_1, \quad (45)$$

which is independent of the SSC chosen (i.e. $\kappa = 0$ or $\kappa = 1/2$).

2. Radiation

No spin

The relevant diagram for the \mathcal{C}^2 contribution to the emission from non-spinning sources is given in fig. 7,⁸ which gives, see app. C 1 a for details,

$$L_{fig.7} = 336 \frac{G_N^2 m_1^2 m_2}{\Lambda^6 r^8} r^i r^j \frac{\ddot{\sigma}_{ij}}{2m_{Pl}} + 1 \leftrightarrow 2 = 336 \frac{G_N^2 \eta M^3}{(\Lambda r)^6} n^i n^j \frac{\ddot{\sigma}_{ij}}{2m_{Pl}}, \quad (46)$$

with $n^i \equiv \frac{r^i}{r}$, where to simplify the calculations we work in the Transverse Traceless (TT) gauge, which is valid only for the radiative field (i.e. on-shell in vacuum) and which enables to write $\ddot{\sigma}_{ij} = \nabla^2 \sigma_{ij} = 2R_{0ij0} m_{Pl}$ and $\dot{\sigma}_{ij,k} - \dot{\sigma}_{ik,j} = 2R_{0ijk} m_{Pl}$.

To express the leading radiative coupling in terms of the quadrupole one needs to combine eq. (46) with the contribution coming from the modified equation of motion (42), that enters the game when expressing the radiative coupling (9) in terms of quadrupole derivatives, see eq. (A2) for details. In total one has

$$L_{rad-\Lambda} = \left[\frac{d^2}{dt^2} \left(\frac{Q^{ij}}{2} + 336 \frac{G_N^2 \eta M^3}{(\Lambda r)^6} n^i n^j \right) - 2304 \frac{G_N^3 M^4 \eta (1 - 2\eta)}{\Lambda^6 r^9} n^i n^j \right] \frac{\sigma_{ij}}{2m_{Pl}}. \quad (47)$$

Beside the shift in the quadrupole coupling given by (46), we see that the non-GR structure of our effective theory, via non-conservation of the energy-momentum tensor, introduces terms in radiative interaction which do not have a multipolar structure, as the last term in square bracket in eq.(47). In terms of PN scaling, the Λ dependent terms in (47) are of the same order (remember that $\frac{d}{dt} \sim \frac{1}{t} \sim v/r$): $2\text{PN} \times (\Lambda r)^{-6}$.

Spin

The contribution to radiation emission processes introduced by the quartic interaction due to the \mathcal{C}^2 term can be distinguish in magnetic and electric ones. Contrarily from the non-spinning case, the spinning LO emission process is of *magnetic* type, and described by the processes reported in fig. 8, the ones of electric type are reported in fig. 9 and are $O(v)$ with respect to the former.

Indeed, as it can be seen from the scaling of the world-line (24) and bulk (40) couplings, the processes in fig. 8 give a contribution to the *magnetic* quadrupole which is $2\text{PN} \times (\Lambda r)^{-6}$

⁸ Note that we obtain one fourth of the result of (6.6) of [6].

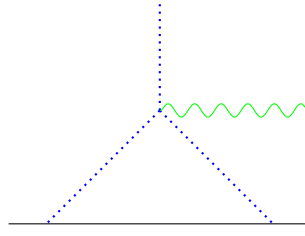


Figure 7: Leading \mathcal{C}^2 correction to the emission process for non-spinning sources. Blue dotted lines are longitudinal modes exchanged between the sources, green wavy line the radiative gravitational mode.

order with respect to the leading GR magnetic quadrupole, whereas the electric emission processes in fig. 9 contribute at order $2.5\text{PN} \times (\Lambda r)^{-6}$ with respect to the leading electric quadrupole in GR, see fig. 2: as a result the contribution from \mathcal{C}^2 terms to the radiation flux F in eq. (15) from the magnetic and the electric quadrupole is of the same order, since for the spin-less part $J_{ij} \sim v \times Q_{ij}$.

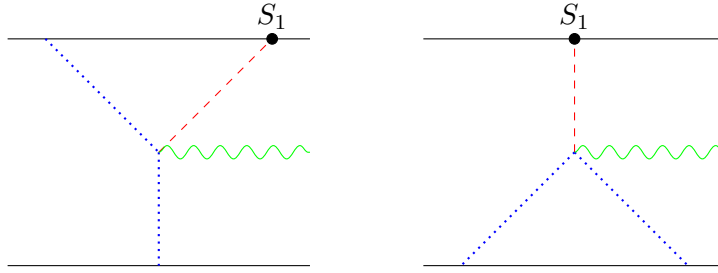


Figure 8: Diagrams representing the leading *magnetic* contribution to radiation emission process from \mathcal{C}^2 interaction, generated by bulk terms $\sim (\partial_i \partial_j \phi)^2 \times \partial_i \partial_j A_k R^{0ijk}$. Blue dotted lines represent ϕ propagators, red dashed for A_i , green wavy for σ_{ij} .

The diagram in fig. 8 represents the linear-in-spin \mathcal{C}^2 contributions to the magnetic quadrupole, giving, see app. C 2 a for details,

$$\mathcal{L}_{fig.8} = \frac{576}{(\Lambda r)^6} \frac{G_N^2 m_2 (m_1 + m_2)}{r^2} (S_1^i r^j + S_1^j r^i) \frac{1}{2} \epsilon_{ikl} R_{0jkl}, \quad (48)$$

which corrects the magnetic quadrupole according to

$$J^{ij}|_S = \frac{3}{4} (S_1^i r^j + S_1^j r^i)_{TF} \times \left(1 + \frac{768 G_N^2 m_1 M}{\Lambda^6 r^8} \right) + 1 \leftrightarrow 2, \quad (49)$$

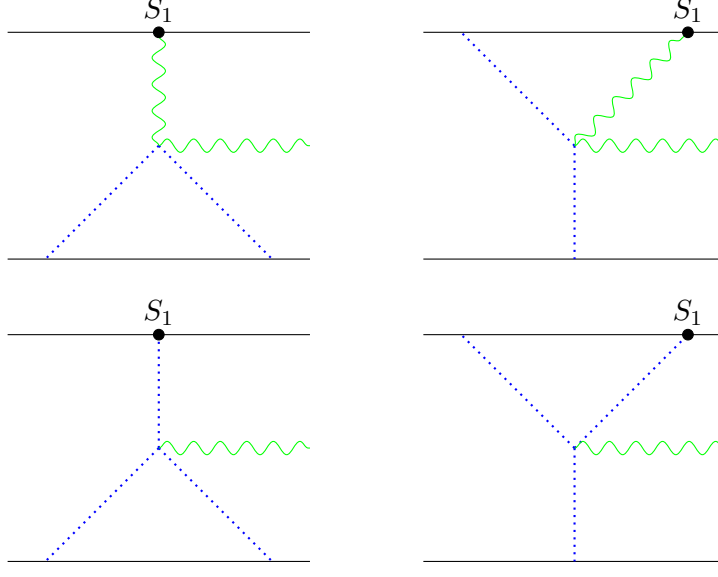


Figure 9: Diagrams representing the leading *electric* contribution to radiation emission process from \mathcal{C}^2 interaction, generated by bulk terms $\sim (\partial_i \partial_j \phi)^2 (\partial_i \partial_j \phi R_{0i0j} + \partial_i \partial_j \sigma_{kl} R_{ikjl})$. Blue dotted lines represent ϕ propagators, red dashed for A_i , green wavy for σ .

which is again a $2\text{PN} \times (\Lambda r)^{-6}$ correction to the LO.

From fig. 9 one gets the linear-in-spin \mathcal{C}^2 corrections to the electric quadrupole

$$\mathcal{L}_{fig.9} = \frac{96}{(\Lambda r)^6} \frac{G_N^2 m_2}{r^2} \left[(5m_1 + 8m_2) r^i \left(\vec{S}_1 \times \vec{r} \right)^j \frac{\vec{r} \cdot \vec{v}_1}{r^2} + (7 + 8\kappa) (m_1 + m_2) r^i \left(\vec{S}_1 \times \vec{v}_1 \right)^j \right. \quad (50) \\ \left. - (m_1 + 4m_2) v_1^i \left(\vec{S}_1 \times \vec{r} \right)^j + 4(1 + \kappa) (5m_1 + 8m_2) r^i r^j \left(\vec{S}_1 \cdot (\vec{r} \times \vec{v}_1) \right) \right] R_{0i0j},$$

which modifies the linear-in-spin part of the electric quadrupole to

$$I_{ij}|_{S_1} = \left\{ \left(\vec{v}_1 \times \vec{S}_1 \right)^i r^j \left[2\kappa + \frac{2}{3} - \frac{96}{(\Lambda r)^6} \frac{G_N^2 M m_2}{r^2} (7 + 8\kappa) \right] \right. \\ \left. + \left(\vec{r} \times \vec{S}_1 \right)^i v^j \left(-\frac{4}{3} + \frac{96}{(\Lambda r)^6} \frac{G_N^2 m_2 (m_1 + 4m_2)}{r^2} \right) \right. \\ \left. + \frac{96}{(\Lambda r)^6} \frac{G_N^2 m_2 (5m_1 + 8m_2)}{r^2} \left[4(1 + \kappa) r^i r^j \left(\vec{S}_1 \cdot (\vec{r} \times \vec{v}_1) \right) + r^i \left(\vec{S}_1 \times \vec{r} \right)^j \frac{(\vec{r} \cdot \vec{v}_1)}{r^2} \right] \right\}_{TF}. \quad (51)$$

B. $\mathcal{C}\tilde{\mathcal{C}}$

The $\tilde{\mathcal{C}}$ term violates both parity and time-reversal invariance, the explicit expression of $\tilde{\mathcal{C}}$ and $\mathcal{C}\tilde{\mathcal{C}}$, limited to the terms with lower number of time derivatives of interest for this work,

are

$$\tilde{\mathcal{C}} \simeq 4 \frac{\epsilon_{jkl}}{m_{Pl}^2} \left[-4 (\partial_i \partial_j \phi) (\partial_i \partial_k A_l) + \ddot{\sigma}_{ij} (\partial_i \partial_k A_l) + (\partial_k \partial_m \sigma_{il}) \partial_j (\partial_i A_m - \partial_m A_i) - 4 (\partial_i \partial_j \phi) \partial_k \dot{\sigma}_{il} \right], \quad (52)$$

$$\mathcal{C}\tilde{\mathcal{C}} \simeq 32 \frac{\epsilon_{jkl}}{m_{Pl}^4} (\partial_m \partial_n \phi) (\partial^m \partial^n \phi) \left[-4 (\partial_i \partial_j \phi) (\partial_i \partial_k A_l) + \ddot{\sigma}_{ij} (\partial_i \partial_k A_l) + (\partial_k \partial_m \sigma_{il}) \partial_j (\partial_i A_m - \partial_m A_i) - 4 (\partial_i \partial_j \phi) \partial_k \dot{\sigma}_{il} \right]. \quad (53)$$

1. Potential

No spin

The $\mathcal{C}\tilde{\mathcal{C}}$ term violates parity and time reversal, and its contribution to the conservative potential vanishes at all orders in the spin-less case, as this interaction involves a Levi-Civita tensor which has to be contracted with three linearly independent vectors to generate a scalar potential. However for a non-spinning binary system all vectors available lie in the orbital plane, hence the $\mathcal{C}\tilde{\mathcal{C}}$ contribution to the potential vanishes.

Spin

In the spinning case diagrams in fig. 10 give, see app. B 2 b for details,

$$\Delta V_{\Lambda_- S_1} = -\frac{442368}{11} \frac{G_N^3 m_1^2 m_2}{r^5 (\Lambda_- r)^6} \vec{r} \cdot \vec{S}_1 \quad (54)$$

which is a $1.5\text{PN} \times (\Lambda_- r)^{-6}$ correction with respect to the leading spin term in the potential eq. (25), the half-integer relative order due to parity violation nature of the term, modifying the spin equation of motion per

$$\Delta \left[\frac{d\vec{S}_1}{dt} \right]_{\Lambda_-} = -\frac{442368}{11} \frac{G_N^3 m_1^2 m_2}{r^5 (\Lambda_- r)^6} \vec{r} \times \vec{S}_1, \quad (55)$$

which induces an explicitly time-dependent perturbation into spin equation of motion, with the period of periodic perturbation being equal to the binary orbital period. This is a distinctive effect generated by the parity violating Lagrangian which is qualitative different from other modifications.

2. Emission

No spin

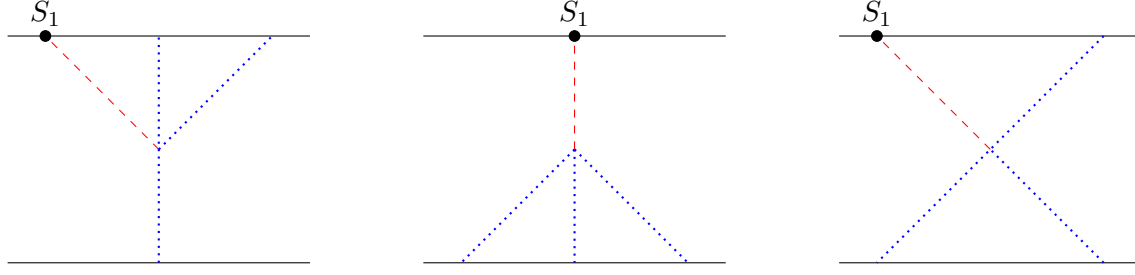


Figure 10: Diagrams representing the leading corrections to the spinning potential from $\mathcal{C}\tilde{\mathcal{C}}$ interactions (blue dotted lines represent ϕ propagators, red dashed A_i ones) at 2PN order with respect to leading GR behaviour. Only the first diagram is non-vanishing.

The parity violating term under consideration couples at lowest order to the magnetic part of the Riemann via an electric term in fig. 11 giving a coupling to radiative field [6], see app. III B 2 for details:

$$L_{rad-\Lambda_-} = -\frac{672}{(\Lambda_- r)^6} \frac{G_N^2 m_1 m_2^2}{r^2} r^i r^j \mathcal{B}_{ij} + 1 \leftrightarrow 2. \quad (56)$$

Note that since at leading order \mathcal{B}_{ij} couples to $J_{ij} = \frac{1}{2} \mu x_k v_l \epsilon^{mkl} (\delta^{mi} x^j + \delta^j_m x^i)$, eq.(56) represents a 1.5PN electric correction to the magnetic quadrupole.

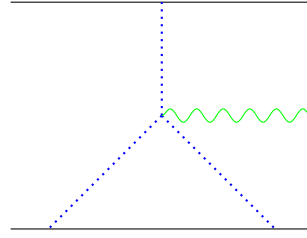


Figure 11: Diagram giving the LO effect of $\mathcal{C}\tilde{\mathcal{C}}$ on the radiation emission for the non-spinning case.

Spin

The diagrams giving the $\mathcal{C}\tilde{\mathcal{C}}$ contribution to radiation in the spinning case are reported in fig. 12, see app. C 2 b for details, and they give

$$L_{rad-\Lambda_- S_1} = 192 \frac{G_N^2 m_2}{r^2 (\Lambda_- r^6)} \left[(8m_2 + 3m_1) \left(r^i S_1^j - n^i n^j (\vec{r} \cdot \vec{S}_1) \right) - 3 \left(\frac{m_1}{2} + m_2 \right) r^i S_1^j \right] \mathcal{E}_i \quad (57)$$

representing a $1.5PN \times (\Lambda_- r)^{-6}$ magnetic type correction to the spin-dependent electric quadrupole which can be read from eq. (38).

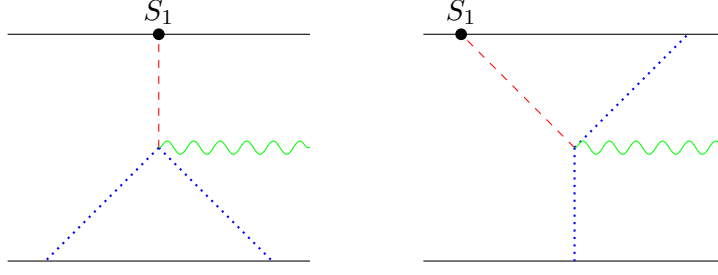


Figure 12: Diagram giving the LO effect of $\tilde{\mathcal{C}}\tilde{\mathcal{C}}$ on the radiation emission for the spinning case.

C. $\tilde{\mathcal{C}}^2$

While the $\tilde{\mathcal{C}}$ term violates parity, the $\tilde{\mathcal{C}}^2$ does not and its expression is given by the square of (52).

1. Potential

No spin

The potential interaction mediated by $\tilde{\mathcal{C}}^2$ vanish in the static limit and it is v^2 with respect to the one mediated by the \mathcal{C}^2 , i.e. a 3PN correction to the Newtonian potential and it will not be computed here.

Spin

The LO potential mediated by the $\tilde{\mathcal{C}}^2$ interaction in the spinning case is given by the processes in fig. 13 with the total result, see app. B 2 c for details,

$$L_{pot-\tilde{\Lambda}S_1} = 13824 \frac{G_N m_1^2 m_2}{r^5 \tilde{\Lambda}^6} [\vec{r} \times (\vec{v}_1 - 2\vec{v}_2)] \cdot \vec{S}_1 \quad (58)$$

This contribution is analogous to the one of the \mathcal{C}^2 term and it introduces a correction to the spin equation of motion

$$\Delta \left[\frac{d\vec{S}_1}{dt} \right]_{\tilde{\Lambda}} = \frac{6912}{\tilde{\Lambda}^6} \frac{G_N^3 m_1^2 m_2 (m_1 + 2m_2)}{Mr^5} \vec{L} \times \vec{S}_1, \quad (59)$$

which is analogous to the \mathcal{C}^2 case eq. (45).

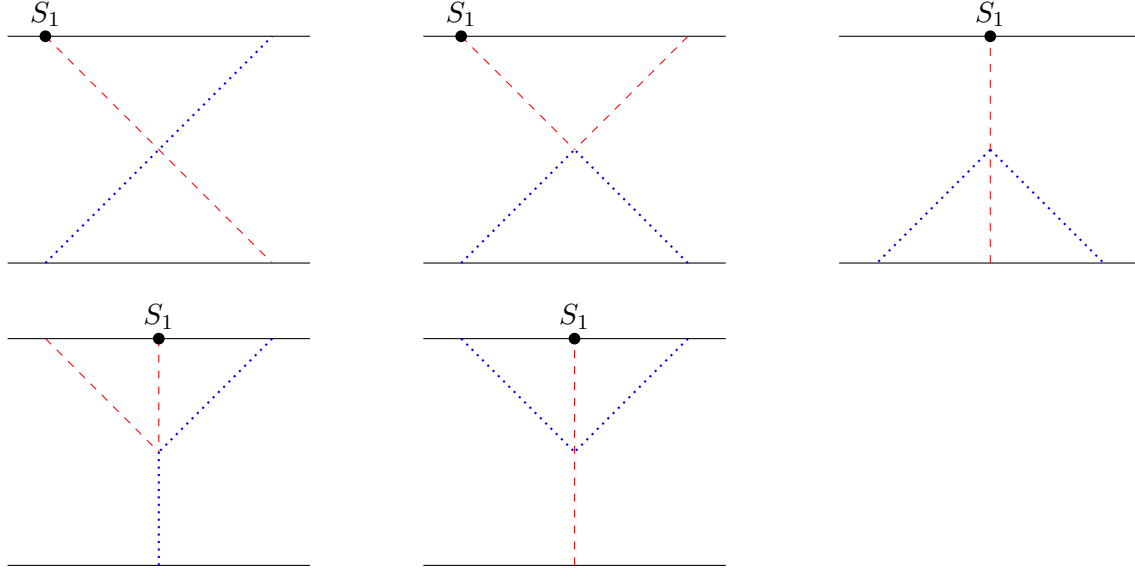


Figure 13: Feynman diagrams representing the correction to the spinning potential mediated by the $\tilde{\mathcal{C}}^2$ bulk interaction. Diagrams must be supplemented with their mirror images under $m_1 \leftrightarrow m_2$. The first three diagrams vanish.

2. Emission

No spin

The radiative interaction due to the $\tilde{\mathcal{C}}^2$ term are v^2 with respect to the one mediated by the \mathcal{C}^2 , i.e. a 3PN correction to the quadrupole formula and it will not be computed here.

Spin

From fig. 14, see app. C 2 c for details,

$$L_{rad-\tilde{\Lambda}S_1} = -\frac{G_N^2 m_1 m_2}{r^2} \frac{48}{(\tilde{\Lambda}r)^6} \left\{ 8n^i n^j [(\vec{r} \times \vec{v}) \cdot \vec{S}_1] - 8n^i (\vec{n} \cdot \vec{v}) (\vec{S}_1 \times \vec{r})^j + 6r^i (\vec{S}_1 \times \vec{v}) + v^i (\vec{S}_1 \times \vec{r})^j \right\} \mathcal{E}_{ij}. \quad (60)$$

IV. DISCUSSION

Following the parametrisation of short-distance gravity modification introduced in [6], we applied the effective field theory methods of non-relativistic General Relativity [7] to re-derive in this modified gravity model the energy and luminosity functions of a compact

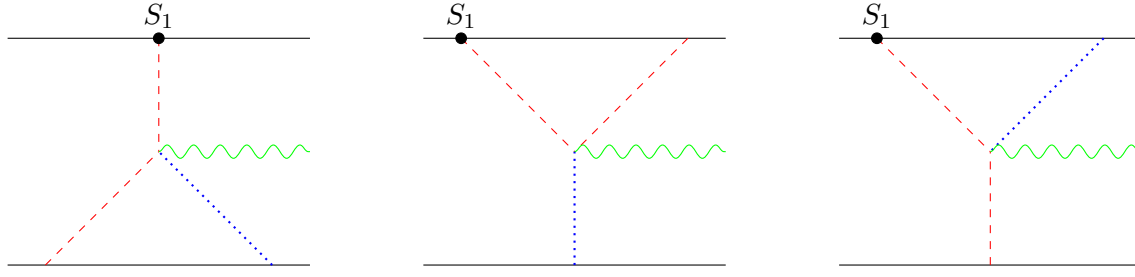


Figure 14: Feynman diagrams representing the correction to the linear-in-spin radiation emission mediated by the $\tilde{\mathcal{C}}^2$ bulk interaction. Diagrams must be supplemented with their mirror images under $m_1 \leftrightarrow m_2$.

two-body system, which are the ingredients to compute the phase of gravitational waves observed routinely since the year 2015 by the gravitational wave observatories LIGO and Virgo. We have extended these results to the linear-in-spin case, also deriving the spin precessing equations obtained from the same modifications to General Relativity.

Whatever physical quantity is being considered (2-body potential, luminosity, gravitational wave phasing, spin equation of motion), the corrections due to the quartic interactions introduced by the extra terms of the type Riemann to the fourth power can be classified as 2PN order in the post-Newtonian approximation times a factor $(\Lambda r)^{-6}$ (being Λ the generic short-distance scale introduced by the quartic curvature terms and r the typical source size) with respect to leading order for parity (and time-reversal) preserving interactions, and 1.5 PN (again times $(\Lambda r)^{-6}$) for parity-violating corrections for spinning systems.

For spins however we have to consider that the high curvature corrections considered affect the phasing formula from 1.5PN order on-wards, hence 1.5PN with respect to leading order, as they occur in the parity-violating case, means 3PN in absolute terms, times the usual $(\Lambda r)^{-6}$ factor.

Current limits set by LIGO/Virgo detections on 2PN and 3PN phasing terms [29, 30] require them to be within $\sim 10\%$ of the value predicted by General Relativity, giving a mild bound on $\Lambda \gtrsim 1/r$, with typical r for LIGO/Virgo detections of the order of ~ 10 km, which translated to an energy scale is $\sim 10^{-12}$ eV.

Other tests are possible via *geodetic precession*, i.e. relativistic spin precession which in General Relativity is caused at leading order by the spin-orbit coupling, that has been observed in the spin of double pulsar PSR J0737-3039 [31–33] and it is currently in agreement

with the value predicted by General Relativity at 13% level.

For the gravitational model under study here, the \mathcal{C}^2 and \mathcal{C}^2 terms give rise to corrections of the order $v^4 \times (\Lambda r)^{-6}$ to the spin precessing equations, as reported in eqs. (45,59), with the typical orbital velocity of binary pulsars being $v \sim 10^{-3}$.

Note however the presence in the spin precession equation of a term $\sim \vec{r} \times \vec{S}_1$ in eq. (55), being r the orbital radius, at the 1.5PN level in the parity violating case of \mathcal{CC} , inducing an oscillation at the orbital frequency $\sim v/r$ on the top of the leading precession effect which has frequency v^5/r . In General Relativity the spin equations of motion at next-to-leading order have a term quadratic in the \vec{r} vector which can produce nutation of the spin at a frequency twice the orbital frequency, but the presence of a modulation at the orbital frequency would be a smoking gun of the parity violating term $\vec{r} \times \vec{S}_1$ in the spin precession equation. The magnitude of this effect is suppressed by $v^3 \times (\Lambda r)^{-6}$ with respect to the leading order precession equation.

Overall, we have extended the analysis of [6] on the effect that high curvature term have on binary systems to include linear-in-spin effects on the gravitational phasing an the spin precession equations, the latter being the most important test-bed of gravity for spinning systems.

Acknowledgements

The authors wish to thank Shao Lijing for useful correspondence. The work of ANL is financed in part by the Coordenação de Aperfeiçoamento de Pessoal de Nível Superior - Brasil (CAPES) - Finance Code 001. RS is partially supported by CNPq. RS would like to thank ICTP-SAIFR FAPESP grant 2016/01343-7.

Appendix A: Derivation of multipolar radiative coupling in GR

The first diagram in fig. 2 can be read directly from the Lagrangian (6), the second one needs the $\phi^2\sigma$ Lagrangian bulk term which appears in eq. (4)

$$L_{rad-2b} = \frac{m_1 m_2}{8m_{Pl}^2} \int \frac{d^3 k}{(2\pi)^3} \frac{k^i k^j}{k^4} e^{ik^i r_i} = -\frac{G_N m_1 m_2 r^i r^j}{2r^3} \frac{\sigma_{ij}}{m_{Pl}}, \quad (A1)$$

where a term proportional to the trace of σ has been neglected, since it does not contribute to radiation in the TT gauge. Using the Newtonian equations of motion (10) one gets

$$\begin{aligned} L_{rad-LO} &= m_1 \left(v_1^i v_1^j - \frac{G_N m_2}{2r^3} r^i r^j \right) \frac{\sigma_{ij}}{2m_{Pl}} + 1 \leftrightarrow 2 \\ &= \left[m_1 v_1^i v_1^j + \frac{m_1}{2} \ddot{x}_1^i x_1^j + \frac{m_2}{2} x_2^i \ddot{x}_2^j - \left(\frac{G_N m_2}{2r^3} r^i r^j + \frac{m_1}{2} \ddot{x}_1^i r^j \right) \right] \frac{\sigma_{ij}}{2m_{Pl}} + 1 \leftrightarrow 2 \\ &= \left\{ \frac{m_1}{4} \frac{d^2}{dt^2} (x_1^i x_1^j) + \frac{m_2}{4} \frac{d^2}{dt^2} (x_2^i x_2^j) - \left[\frac{G_N m_1 m_2}{2r^3} r^i r^j + \frac{m_1 m_2}{4M} (\dot{r}^i r^j + r^i \dot{r}^j) \right] \right\} \frac{\sigma_{ij}}{m_{Pl}}, \end{aligned} \quad (\text{A2})$$

from which one obtains the standard result (11) observing that the term in square brackets in the last line is $O(Spin)$ on the equation of motions.

The usual textbook procedure to derive source multipole coupling for an extended source (like a binary system, extended over a volume V) whose size $r \ll \lambda_{gw}$, being λ_{gw} the GW wavelength, is the following:

$$\begin{aligned} \mathcal{S}_{mult} &= \frac{1}{2} \int dt \int d^3x T^{\mu\nu}(t, \vec{x}) h_{\mu\nu}(t, \vec{x}) \simeq \\ &\quad \frac{1}{2} \int dt \left\{ \left(\int_V T^{00} \right) h_{00}(t, 0) + \left[2 \left(\int_V T_{0i} \right) h_{0i} + \left(\int_V T^{00} x^i \right) h_{00,i}(t, 0) \right] + \right. \\ &\quad \left[\left(\int_V T^{ij} \right) h_{ij} + \left(\int_V T_{0i,j} \right) (h_{0i,j}(t, 0) + h_{0j,i}(t, 0)) + \frac{1}{2} \left(\int_V T_{00} x^i x^j \right) h_{00,ij}(t, 0) \right] \\ &\quad \left. + \left(\int_V T_{0i,j} \right) (h_{0i,j} - h_{0j,i}) + \left(\int_V T^{ij} x^k \right) h_{ij,k} + \dots \right\}, \end{aligned} \quad (\text{A3})$$

where the notation $\int d^3x = \int_V$ for brevity. Note that this Taylor expansion is actually an expansion in $r/\lambda_{gw} \sim v$ where v is the source internal velocity.

Using repeatedly the energy-momentum conservation in the form $\dot{T}^{\mu 0} = -T^{\mu i}_{,i}$ one can derive

$$\begin{aligned} \int_V T^{ij} &= \frac{1}{2} \frac{d^2}{dt^2} \left(\int_V T^{00} x^i x^j \right) \equiv \frac{1}{2} \ddot{Q}^{ij}, \\ \int_V T^{0i} &= -\frac{d}{dt} \left(\int_V T^{00} x^i \right), \\ \int_V T^{ij} x^k &= \frac{1}{3} \int_V (T^{ij} x^k + T^{ki} x^j + T^{jk} x^i) + \frac{1}{3} \int_V (2T^{ij} x^k - T^{ik} x^j - T^{jk} x^i), \\ &= \frac{1}{6} \frac{d^2}{dt^2} \left(\int_V T^{00} x^i x^j x^k \right) + \frac{1}{3} \frac{d}{dt} \left[\int_V (T^{0i} x^k x^j + T^{0j} x^k x^i - 2T^{0k} x^i x^j) \right], \end{aligned} \quad (\text{A4})$$

The coupling $T^{ij} h_{ij}$ hence gives rise to the electric quadrupole coupling $\frac{1}{2} \ddot{Q}^{ij} R_{0i0j}$ term, where at linear order in terms of the Kaluza-Klein fields ϕ, A_i, σ_{ij}

$$R_{0i0j} \simeq \frac{1}{2m_{Pl}} \left(\ddot{\sigma}_{ij} - \dot{A}_{i,j} - \dot{A}_{j,i} - \phi_{,ij} - \delta_{ij} \frac{\ddot{\phi}}{d-2} \right) + O(h^2). \quad (\text{A5})$$

Moreover defining

$$\begin{aligned} O^{ijk} &\equiv \int_V T^{00} x^i x^j x^k, \\ J^{ij} &\equiv \frac{1}{2} \int_V T^0_l x_k (x^i \epsilon^{jkl} + x^j \epsilon^{ikl}), \end{aligned} \quad (\text{A6})$$

and with the use of the identity

$$\begin{aligned} (T^{0i} x^k x^j - T^{0k} x^i x^j) \sigma_{ij,k} &= T^{0m} x^n x^j (\delta_m^l \delta_n^k - \delta_m^k \delta_n^l) \sigma_{lj,k} \\ &= -\epsilon_{imn} x^m T^{0n} x^j \frac{1}{2} \epsilon^{ikl} (\sigma_{kj,l} - \sigma_{lj,k}) \end{aligned} \quad (\text{A7})$$

and the definition of the magnetic part of the Riemann tensor

$$\mathcal{B}_{ij} = \frac{1}{2} \epsilon_{ikl} R_{0jkl} \simeq \frac{1}{4m_{Pl}} \epsilon_{ikl} \left[\dot{\sigma}_{jk,l} - \dot{\sigma}_{jl,k} + A_{l,jk} - A_{k,jl} + \frac{1}{d-2} (\dot{\phi}_{,k} \delta_{jl} - \dot{\phi}_{,l} \delta_{jk}) \right], \quad (\text{A8})$$

one finds explicitly the magnetic and electric quadrupole and electric octupole gravitational couplings of eq. (14).

At the next order in eq. (A3), i.e electric exadecapole and magnetic octupole, one has the following identity, see [34] for an explicit Lagrangian treatment or [15] for general derivation of the multipole expansion,

$$\begin{aligned} \frac{1}{4} \int_V T^{ij} x^k x^l &= \frac{1}{4} \times \frac{1}{6} \int_V (T^{ij} x^k x^l + T^{li} x^j x^k + T^{kl} x^i x^j + T^{jk} x^l x^i + T^{ik} x^j x^l + T^{jl} x^i x^k) \\ &+ \frac{1}{4} \times \frac{1}{2} \int_V (T^{ij} x^k x^l - T^{kl} x^i x^j) \\ &+ \frac{1}{4} \times \frac{1}{6} \int_V (2T^{ij} x^k x^l + 2T^{kl} x^i x^j - T^{li} x^j x^k - T^{jk} x^l x^i - T^{ik} x^j x^l - T^{jl} x^i x^k), \end{aligned} \quad (\text{A9})$$

where the first line contains the electric exadecapole $l = 4$, the second line contains the magnetic octupole $l = 3$ and the third line is a contribution to the electric quadrupole ($l = 2$). From the third line of (A9) one gets the multipole coupling

$$\begin{aligned} &\frac{1}{4} \left(\int_V T^{ij} x^k x^l \right) \Big|_{(\text{A9})3^{rd} \text{line}} \sigma_{ij,kl} \\ &= \frac{1}{4} \times \frac{1}{12} (\epsilon_{ikm} \epsilon_{jln} + \epsilon_{ilm} \epsilon_{jkn} + \epsilon_{jkm} \epsilon_{iln} + \epsilon_{jlm} \epsilon_{ikn}) \epsilon_{rum} \epsilon_{svn} \int_V (T^{rs} x^u x^v) \sigma_{ij,kl} \\ &= \frac{1}{12} \epsilon_{rum} \epsilon_{svn} \int_V (T^{rs} x^u x^v) \frac{\ddot{\sigma}_{mn}}{m_{Pl}} \\ &= \frac{1}{12} \int_V (T^{ll} x^m x^n + T^{mn} r^2 - T^{ml} x^n x^l - T^{nl} x^l x^m) \ddot{\sigma}_{mn}, \end{aligned} \quad (\text{A10})$$

where the relationship⁹

$$R_{ijkl} = \epsilon_{ijm} \epsilon_{klm} R_{0m0n} \quad (\text{A11})$$

⁹ Note the different sign in eq. (A11) and in eq. (60) of [34], where a “mostly minus” metric signature is used.

has been used, which is valid for the radiative field (i.e. on shell in vacuum). To collect all the electric quadrupole contributions from second order multipole expansions one must add to eq. (A10) the terms obtained by subtracting traces from the first and second line of (A9):

$$\begin{aligned} \frac{1}{4} \left(\int_V T^{ij} x^k x^l \right) \Big|_{Tr-Exa} \sigma_{ij,kl} &= \frac{1}{4} \times \frac{1}{42} \int_V (T^{ij} r^2 + T^{ll} x^i x^j + 2(T^{il} x^l x^j + T^{jl} x^l x^i)) \ddot{\sigma}_{ij}, \\ \frac{1}{4} \left(\int_V T^{ij} x^k x^l \right) \Big|_{Tr-Oct} \sigma_{ij,kl} &= -\frac{1}{4} \times \frac{1}{6} \int_V (T^{ll} x^i x^j - T^{ij} r^2) \ddot{\sigma}_{ij}, \end{aligned} \quad (\text{A12})$$

where we used that the gravitational field is on-shell and in vacuum (i.e. $\ddot{\sigma}_{ij} = \nabla^2 \sigma_{ij}$ and $\sigma_{ij,j} = 0$).

In the standard approach one then uses repeatedly the energy momentum conservation equation to derive

$$\begin{aligned} \int_V (T^{ij} r^2 + T^{ll} x^i x^j) &= \int_V \left[\left(-\frac{1}{2} \ddot{T}^{00} r^2 + 2\dot{T}^{0l} x^l \right) x^i x^j + \left(\dot{T}^{i0} x^j + \dot{T}^{j0} x^i \right) r^2 \right. \\ &\quad \left. - 2(T^{im} x^m x^j + T^{jm} x^m x^i) \right], \\ \int_V (T^{il} x^l x^j + T^{jl} x^l x^i) &= \int_V \left[\left(\dot{T}^{0l} x^l - T^{ll} \right) x^i x^j \right], \\ \int_V (\dot{T}^{i0} x^j + \dot{T}^{j0} x^i) r^2 &= \int_V \left(\ddot{T}^{00} r^2 x^i x^j - 2\dot{T}^{0l} x^l x^i x^j \right), \end{aligned} \quad (\text{A13})$$

from which one recovers the standard form of the radiative electric quadrupole involved in the GR electric quadrupole coupling (11) (valid up to $O(v^2)$ with respect to LO)

$$\frac{1}{2} I^{ij} R_{0i0j} = \frac{1}{2} R_{0i0j} \int_V \left(T^{00} + T^{ll} - \frac{4}{3} \dot{T}^{0l} x^l + \frac{11}{42} \ddot{T}^{00} r^2 \right) x^i x^j. \quad (\text{A14})$$

However since we are using non-GR equation of motions to derive the main results of this paper, in particular in secs. III A 2, III B 2 and III C 2, we will use the GR-equivalent multipole expanded coupling (A3)

$$\begin{aligned} \frac{1}{2} \int_V T^{ij}(t, \vec{x}) \frac{\sigma_{ij}(t, \vec{x})}{m_{Pl}} \\ \simeq \frac{\sigma_{ij}(t, 0)}{2m_{Pl}} \int_V \left[T^{ij} + \frac{1}{7} \frac{d^2}{dt^2} \left(\frac{2}{3} T^{ll} x^i x^j + \frac{11}{6} T^{ij} r^2 - T^{il} x^l x^j - T^{jl} x^l x^i \right) \right]. \end{aligned} \quad (\text{A15})$$

One can check explicitly that eqs. (A14) and (A15) are equivalent in GR on the equation of motions, in particular for the spinning case by using in eq. (A15) the energy momentum tensor T_{ij} derived via the sum of eqs. (33) and (34), the equation of motion (30) and (A2), and in eq. (A14) the LO T^{0i} and T^{ij} which can be read directly from the point-particle Lagrangian (24).

Appendix B: Higher order curvature contributions to the conservative Lagrangian

1. No Spin

$$a. \quad \mathcal{C}^2$$

The amplitudes corresponding to the diagrams in fig. 5 are

$$\begin{aligned} A_{fig. 5a} &= \frac{m_1 m_2^3}{64 m_{Pl}^4} \int_{\mathbf{p}, \mathbf{k}_1, \mathbf{k}_2} e^{i \vec{p} \cdot \vec{r}} \frac{\left[\vec{k}_2 \cdot (\vec{k}_1 - \vec{k}_2) \right]^2 \left[\vec{p} \cdot (\vec{p} - \vec{k}_1) \right]^2}{p^2 (p - k_1)^2 (k_1 - k_2)^2 k_2^2} = -256 \frac{G_N^3 m_1 m_2^3}{\Lambda^6 r^9} \\ A_{fig. 5b} &= \frac{m_1^2 m_2^2}{64 m_{Pl}^4} \int_{\mathbf{p}, \mathbf{k}_1, \mathbf{k}_2} e^{i \vec{p} \cdot \vec{r}} \times \\ &\quad \frac{\left[\vec{k}_1 \cdot (\vec{p} - \vec{k}_1) \right]^2 \left[\vec{k}_2 \cdot (\vec{p} - \vec{k}_2) \right]^2 + 2 \left(\vec{k}_1 \cdot \vec{k}_2 \right)^2 \left[(\vec{p} - \vec{k}_1) \cdot (\vec{p} - \vec{k}_2) \right]^2}{\left(\vec{p} - \vec{k}_1 \right)^2 \vec{k}_1^2 \left(\vec{p} - \vec{k}_2 \right)^2 \vec{k}_2^2} = 0, \end{aligned} \quad (B1)$$

which can be computed by repeated use (and differentiations) of the “kyte” integral

$$\int_{\mathbf{k}} \frac{1}{k^{2a} (p - k)^{2b}} = \frac{\Gamma(d/2 - a) \Gamma(d/2 - b) \Gamma(a + b - d/2)}{(4\pi)^{d/2} \Gamma(a) \Gamma(b) \Gamma(d - a - b)}, \quad (B2)$$

and of the fundamental integral

$$\int_{\mathbf{p}} \frac{e^{i \vec{p} \cdot \vec{r}}}{p^{2a}} = \frac{1}{2^{2a} \pi^{d/2}} \frac{\Gamma(d/2 - x)}{\Gamma(x)}. \quad (B3)$$

2. Spin

a. \mathcal{C}^2

The amplitudes from diagrams in fig. 6, grouped according to the gravitational polarisation attached to the spin, are the following:

$$\begin{aligned}
A_{fig.6-A} &= -\frac{m_1^2 m_2}{16 m_{Pl}^4} \int_{\mathbf{p}, \mathbf{k}_1, \mathbf{k}_2} \frac{e^{i \vec{p} \cdot \vec{r}}}{p^2 (p - k_1)^2 (k_1 - k_2)^2 k_2^2} \times (\vec{k}_2 \cdot \vec{v}_1) \\
&\quad \times \left\{ \left[\vec{p} \cdot (\vec{p} - \vec{k}_1) \right]^2 \left(\vec{k}_1 - \vec{k}_2 \right) \cdot \vec{k}_2 k_2^i (k_1 - k_2)^j \right. \\
&\quad \left. + \left[(\vec{k}_1 - \vec{k}_2) \cdot (\vec{p} - \vec{k}_1) \right]^2 \vec{p} \cdot \vec{k}_2 \frac{1}{2} k_2^i p^j \right\} S_{1ij} \\
&= i \frac{576}{(\Lambda r)^6} \frac{G_N^3 m_1^2 m_2}{r^5} r_i v_{1j} S_1^{ij}, \\
A_{fig.6-\phi} &= -\frac{m_2}{16 m_{Pl}^4} \int_{\mathbf{p}, \mathbf{k}_1, \mathbf{k}_2} \frac{e^{i \vec{p} \cdot \vec{r}}}{p^2 (p - k_1)^2 (k_1 - k_2)^2 k_2^2} \\
&\quad \times \left\{ m_1^2 \left\{ 2 \left[(\vec{k}_1 - \vec{k}_2) \cdot \vec{k}_2 \right]^2 \left[\vec{p} \cdot (\vec{p} - \vec{k}_1) \right]^2 \right. \right. \\
&\quad \left. \left. + \left[(\vec{k}_1 - \vec{k}_2) \cdot (\vec{p} - \vec{k}_1) \right]^2 \left[\vec{p} \cdot \vec{k}_2 \right]^2 \right\} \right. \\
&\quad \left. - m_2^2 \left\{ \vec{p} \cdot (\vec{p} - \vec{k}_1) \right\}^2 \left[\vec{k}_2 \cdot (\vec{k}_1 - \vec{k}_2) \right]^2 \right\} p_i (S_1^{i0} + v_{1j} S_1^{ij}) \\
&= i \frac{2304}{(\Lambda r)^6} \frac{G_N^3 m_2}{r^5} (m_1^2 + m_2^2) (r_i S^{i0} + r_i v_{1j} S_1^{ij}), \\
A_{fig.6-\sigma} &= \frac{m_1^2 m_2}{32 m_{Pl}^6} \int_{\mathbf{p}, \mathbf{k}_1, \mathbf{k}_2} \frac{e^{i \vec{k} \cdot \vec{r}}}{p^2 (p - k_1)^2 (k_1 - k_2)^2 k_2^2} \left\{ \left[(\vec{k}_1 - \vec{k}_2) (\vec{p} - \vec{k}_1) \right]^2 \vec{p} \cdot \vec{k}_2 p^j \right. \\
&\quad \left. + 2 \left[\vec{p} \cdot (\vec{p} - \vec{k}_1) \right]^2 (\vec{k}_1 - \vec{k}_2) \cdot k_2 k_2^j \right\} \vec{k}_2 \cdot \vec{v}_1 k_2^i S_{1ij} \\
&= -i \frac{576}{(\Lambda r)^6} \frac{G_N^3 m_1^2 m_2}{r^5} r_i v_{1j} S_1^{ij},
\end{aligned} \tag{B4}$$

which add up to give the potential

$$V_\Lambda = -\frac{2304}{(\Lambda r)^6} \frac{G_N^3 m_2}{r^5} (m_1^2 + m_2^2) (r_i S^{i0} + r_i v_{1j} S_1^{ij}), \tag{B5}$$

leading via eq. (26) to eq. (45).

b. $\mathcal{C}\tilde{\mathcal{C}}$

The amplitudes from diagrams in fig. 10 are

$$\begin{aligned}
A_{fig.10a} &= \frac{m_1^2 m_2}{8m_{Pl}^6} \int_{\mathbf{p}, \mathbf{k}_1, \mathbf{k}_2} \frac{e^{i\vec{p} \cdot \vec{r}}}{p^2 (p - k_1)^2 (k_1 - k_2)^2 k_2^2} \left\{ \left[(\vec{k}_1 - \vec{k}_2) \cdot \vec{k}_2 \right]^2 \left[\vec{p} \cdot (\vec{p} - \vec{k}_1) \right] p^j \right. \\
&\quad \left. + 2 \left[\vec{p} \cdot \vec{k}_1 \right]^2 \left[(\vec{p} - \vec{k}_1) \cdot (\vec{k}_1 - \vec{k}_2) \right] (k_1 - k_2)^j \right\} (p - k_1)^k \epsilon_{ijk} S_1^{il} \\
&= -i \frac{221184}{11 (\tilde{\Lambda} r)^6} \frac{G_N^3 m_1^2 m_2}{r^5} \epsilon_{ijk} r^i S_1^{jk}, \\
A_{fig.10b} &= \frac{3m_1^2 m_2}{8m_{Pl}^6} \int_{\mathbf{p}, \mathbf{k}_1, \mathbf{k}_2} \frac{e^{i\vec{p} \cdot \vec{r}}}{p^2 (p - k_1)^2 (k_1 - k_2)^2 k_2^2} \\
&\quad \times \left[(\vec{k}_1 - \vec{k}_2) \cdot \vec{k}_2 \right]^2 \left[\vec{p} \cdot (\vec{p} - \vec{k}_1) \right] p^l k_1^j p^k \epsilon_{ijk} S_1^{il} = 0, \\
A_{fig.10c} &= \frac{m_1^2 m_2}{8m_{Pl}^6} \int_{\mathbf{p}, \mathbf{k}_1, \mathbf{k}_2} \frac{e^{i\vec{p} \cdot \vec{r}}}{(p - k_1)^2 k_1^2 (p - k_2)^2 k_2^2} \\
&\quad \times \left\{ \left[\vec{k}_2 \cdot (\vec{p} - \vec{k}_2) \right]^2 \left[(\vec{p} - \vec{k}_1) \cdot \vec{k}_1 \right] k_1^j p^k \right. \\
&\quad \left. + \left(\vec{k}_1 \cdot \vec{k}_2 \right)^2 \left[(\vec{p} - \vec{k}_1) \cdot \vec{k}_2 \right] (p - k_2)^j (p - k_2)^k \right\} \left(\vec{p} - \vec{k}_1 \right)^l \epsilon_{ijk} S_1^{il} = 0,
\end{aligned} \tag{B6}$$

which give the potential in eq. (54).

c. $\tilde{\mathcal{C}}^2$

The amplitudes from the non-vanishing diagrams in fig. 13 are

$$\begin{aligned}
A_{fig.13d} &= i \frac{m_1^2 m_2}{2m_{Pl}^6} \int_{\mathbf{p}, \mathbf{k}_1, \mathbf{k}_2} \frac{e^{i\vec{p} \cdot \vec{r}}}{p^2 (p - k_1)^2 (k_1 - k_2)^2 k_2^2} \\
&\quad \times \left\{ \left[(\vec{p} - \vec{k}_1) \cdot \vec{k}_2 \right] \left[\vec{p} \cdot (\vec{k}_1 - \vec{k}_2) \right] k_2^k p^{k_2} + \left[(\vec{p} - \vec{k}_1) \cdot \vec{p} \right] \left[\vec{k}_2 \cdot (\vec{k}_1 - \vec{k}_2) \right] p^k k_2^{k_2} \right\} \\
&\quad \times (p - k_1)^l (k_1 - k_2)^{l_2} v_1^{j_2} (p - k_1)^i \epsilon_{jkl} \epsilon_{j_2 k_2 l_2} S_1^{ij} \\
&= -i \frac{13824}{11 (\tilde{\Lambda} r)^6} \frac{G_N^3 m_1^2 m_2}{r^5} (\vec{r} \times \vec{v}_1) \cdot \vec{S}_1, \\
A_{fig.13e} &= i \frac{m_1^2 m_2}{m_{Pl}^6} \int_{\mathbf{p}, \mathbf{k}_1, \mathbf{k}_2} \frac{e^{i\vec{p} \cdot \vec{r}}}{p^2 (p - k_1)^2 (k_1 - k_2)^2 k_2^2} \\
&\quad \times v_2^{j_2} k_2^k (k_1 - k_2)^{k_2} (p - k_1)^{l_2} \epsilon_{jkl} \epsilon_{j_2 k_2 l_2} S_1^{ij} \\
&= i \frac{27648}{11 (\tilde{\Lambda} r)^6} \frac{G_N^3 m_1^2}{r^5} (\vec{r} \times \vec{v}_2) \times \vec{S}_1.
\end{aligned} \tag{B7}$$

Appendix C: Higher order curvature contributions to radiative coupling

1. No spin

a. \mathcal{C}^2

The leading correction to radiative coupling is given by the diagram in fig. 7

$$\begin{aligned} A_{fig. 7} &= \frac{m_1 m_2^2}{4 m_{Pl}^4} \int_{\mathbf{p}, \mathbf{k}} e^{i \vec{p} \cdot \vec{r}} \frac{p^i p^j [\vec{k} \cdot (\vec{p} - \vec{k})]^2 + 2 k^i k^j [\vec{p} \cdot (\vec{p} - \vec{k})]^2}{p^2 (p - k)^2 k^2} \times R_{0i0j} \\ &= 336 \frac{G_N^2 m_1 m_2^2}{r^6} n^i n^j R_{0i0j}, \end{aligned} \quad (C1)$$

to which the diagrams obtained under $1 \leftrightarrow 2$ exchange must be added, and terms $\propto \delta^{ij} R_{0i0j}$ which are vanishing on-shell have been neglected.

b. $\mathcal{C}\tilde{\mathcal{C}}$

The diagram in fig. 11 is worth

$$\begin{aligned} A_{fig. 11} &= -i \frac{m_1 m_2^2}{m_{Pl}^4} \int_{\mathbf{p}, \mathbf{k}} \frac{1}{p^2 (p - k)^2 k^2} \left\{ \frac{1}{2} p^i p^j [\vec{k} \cdot (\vec{p} - \vec{k})]^2 + k^i k^j [\vec{p} \cdot (\vec{p} - \vec{k})]^2 \right\} \mathcal{B}_{ij} \\ &= -i \frac{672}{(\tilde{\Lambda} r)^6 r^2} \frac{G_N^2 m_1 m_2^2}{r^2} r^i r^j \frac{1}{2} \epsilon_{ikl} R_{0jkl}. \end{aligned} \quad (C2)$$

2. Spin

a. \mathcal{C}^2

The leading, linear-in-spin corrections to the magnetic quadrupole comes from diagrams in fig. 8 which gives respectively

$$\begin{aligned} A_{fig. 8a} &= i \frac{m_1 m_2}{m_{Pl}^4} \int_{\mathbf{p}, \mathbf{k}} e^{i \vec{p} \cdot \vec{r}} \frac{[\vec{p} \cdot (p - k)]^2}{p^2 (p - k)^2 k^2} k^i k^k k^l \times \epsilon_{jlm} S_1^m R_{0ijk} \\ &\quad 576 \frac{G_N^2 m_1 m_2}{\Lambda^6 r^8} r^i S_1^m \epsilon_{jkm} R_{0ijk}, \\ A_{fig. 8b} &= i \frac{m_2^2}{2 m_{Pl}^4} \int_{\mathbf{p}, \mathbf{k}} e^{i \vec{p} \cdot \vec{r}} \frac{[\vec{k} \cdot (p - k)]^2}{p^2 (p - k)^2 k^2} p^i p^k p^l \times \epsilon_{jlm} S_1^m R_{0ijk} \\ &\quad 576 \frac{G_N^2 m_2^2}{\Lambda^6 r^8} r^i S_1^m \epsilon_{jkm} R_{0ijk}, \end{aligned} \quad (C3)$$

which using Bianchi identity $R_{0ijk} + R_{0kij} + R_{0jki} = 0$ gives eq. (48).

The leading, linear-in-spin electric quadrupole corrections are due to the diagrams in fig. 9 which gives:

$$\begin{aligned}
A_{fig.9a} &= -i \frac{m_2^2}{8m_{Pl}^4} \int_{\mathbf{p}, \mathbf{k}} e^{i\vec{p} \cdot \vec{r}} \frac{[\vec{k} \cdot (p - k)]^2}{p^2 (p - k)^2 k^2} (\vec{p} \cdot v_1) p^j p^k S_1^l \epsilon_{ikl} R_{0i0j} \\
&= 96 \frac{G_N^2 m_2^2}{\Lambda^6 r^8} \left[8 (\vec{r} \cdot \vec{v}_1) r^i (\vec{S}_1 \times \vec{r})^j + 4 v_1^i (\vec{r} \times \vec{S}_1)^j + r^i (\vec{v}_1 \times \vec{S}_1)^j \right] R_{0i0j}, \\
A_{fig.9b} &= i \frac{m_1 m_2}{4m_{Pl}^4} \int_{\mathbf{p}, \mathbf{k}} e^{i\vec{p} \cdot \vec{r}} \frac{[\vec{k} \cdot (p - k)]^2}{p^2 (p - k)^2 k^2} \left[(\vec{k} \cdot v_1) k^j k^k S_1^l \right] \epsilon_{ikl} R_{0i0j} \\
&= 96 \frac{G_N^2 m_1 m_2}{\Lambda^6 r^8} \left[5 (\vec{r} \cdot \vec{v}_1) r^i (\vec{S}_1 \times \vec{r})^j + v_1^i (\vec{r} \times \vec{S}_1)^j + r^i (\vec{v}_1 \times \vec{S}_1)^j \right] R_{0i0j}, \\
A_{fig.9c} &= i \frac{m_2^2}{2m_{Pl}^4} \int_{\mathbf{p}, \mathbf{k}} e^{i\vec{p} \cdot \vec{r}} \frac{[\vec{k} \cdot (p - k)]^2}{p^2 (p - k)^2 k^2} (\vec{k} \cdot v_1) p^i p^j p^l v_1^k S_1^m (1 + \kappa) \epsilon_{klm} R_{0i0j} \\
&= (1 + \kappa) \frac{96}{(\Lambda r)^6} \frac{G_N m_2^2}{r^2} \left(\vec{S}_1 \times (\vec{r} \times \vec{v}_1) + r^i (\vec{v} \times \vec{S}_1)^j \right) \epsilon_{klm} R_{0i0j}, \\
A_{fig.9d} &= i \frac{m_1 m_2}{2m_{Pl}^4} \int_{\mathbf{p}, \mathbf{k}} \frac{[\vec{k} \cdot (p - k)]^2}{p^2 (p - k)^2 k^2} (\vec{k} \cdot v_1) k^i k^j k^l v_1^k S_1^m (1 + \kappa) \epsilon_{klm} R_{0i0j} \\
&= (1 + \kappa) \frac{96}{(\Lambda r)^6} \frac{G_N m_1 m_2}{r^2} \left(\vec{S}_1 \times (\vec{r} \times \vec{v}_1) + r^i (\vec{v} \times \vec{S}_1)^j \right) \epsilon_{klm} R_{0i0j}.
\end{aligned} \tag{C4}$$

b. $\mathcal{C}\tilde{\mathcal{C}}$

The diagrams in fig. 12 give

$$\begin{aligned}
A_{fig.12a} &= i \frac{m_1 m_2^2}{2m_{Pl}^4} \int_{\mathbf{p}, \mathbf{k}} \frac{[(\vec{p} - \vec{k}_1) \cdot k_1]^2}{p^2 (p - k_1)^2 k_1^2} p^j p^r p^k S_1 l r \epsilon_{ikl} R_{0i0j} \\
&= i 192 \frac{G_N^2 m_2^2}{r^2 (\tilde{\Lambda} r^6)} \left[8 \left(r^i S_1^j - n^i n^j (\vec{r} \cdot \vec{S}_1) \right) - 3m_2 \right] r^i S_1^j R_{0i0j} \\
A_{fig.12b} &= i \frac{m_1 m_2^2}{2m_{Pl}^4} \int_{\mathbf{p}, \mathbf{k}} \frac{[\vec{p} \cdot k_1]^2}{p^2 (p - k_1)^2 k_1^2} (p - k_1)^j (p - k_1)^r p^k S_1 l r \epsilon_{ikl} R_{0i0j} \\
&= i 192 \frac{G_N^2 m_2^2}{r^2 (\tilde{\Lambda} r^6)} \left[8 \left(r^i S_1^j - n^i n^j (\vec{r} \cdot \vec{S}_1) \right) - 3m_2 \right] r^i S_1^j R_{0i0j} \\
&= 376 \frac{G_N^2 m_1 m_2}{r^2 (\tilde{\Lambda} r^6)} \left[(r^i S_1^j - n^i n^j) (\vec{r} \cdot \vec{S}_1) - \frac{1}{2} r^i S_1^j \right] R_{0i0j}
\end{aligned} \tag{C5}$$

c. $\tilde{\mathcal{C}}^2$

The three diagrams in fig.14 gives

$$\begin{aligned}
A_{fig.14a} &= -\frac{m_1 m_2^2}{4m_{Pl}^4} \int_{\mathbf{p}, \mathbf{k}} \frac{\left[(\vec{p} - \vec{k}_1) \cdot \vec{k}_1 \right]}{p^2 (p - k_1)^2 k_1^2} p^i p^k k_1^{k_2} p^r (p - k_1)^{l_2} S_1^{lr} v_2^{j_2} \epsilon_{jkl} \epsilon_{j_2 k_2 l_2} R_{0i0j} = 0, \\
A_{fig.14b} &= -\frac{m_1^2 m_2}{4m_{Pl}^4} \int_{\mathbf{p}, \mathbf{k}} \frac{\left[\vec{p} \cdot \vec{k}_1 \right]}{p^2 (p - k_1)^2 k_1^2} p^i p^k p^{k_2} k_1^{l_2} (p - k_1)^r S_1^{lr} v_1^{j_2} \epsilon_{jkl} \epsilon_{j_2 k_2 l_2} R_{0i0j} \\
&= i192 \frac{G_N^2 m_1^2 m_2}{r^2 (\tilde{\Lambda} r)^6} \left\{ 8n^i n^j \left[(\vec{r} \times \vec{v}_1) \cdot \vec{S}_1 \right] - 8n^i (\vec{n} \cdot \vec{v}_1) \left(\vec{S}_1 \times \vec{r} \right)^j \right. \\
&\quad \left. + 6r^i \left(\vec{S}_1 \times \vec{v}_1 \right) + v_1^i \left(\vec{S}_1 \times \vec{r} \right)^j \right\} R_{0i0j}, \\
A_{fig.14c} &= -\frac{m_1^2 m_2}{4m_{Pl}^4} \int_{\mathbf{p}, \mathbf{k}} \frac{\left[\vec{p} \cdot \vec{k}_1 \right]}{p^2 (p - k_1)^2 k_1^2} p^i p^k p^{l_2} k_1^{k_2} (p - k_1)^r S_1^{lr} v_1^{j_2} \epsilon_{jkl} \epsilon_{j_2 k_2 l_2} R_{0i0j} \\
&= -i192 \frac{G_N^2 m_1^2 m_2}{r^2 (\tilde{\Lambda} r)^6} \left\{ 8n^i n^j \left[(\vec{r} \times \vec{v}_2) \cdot \vec{S}_1 \right] - 8n^i (\vec{n} \cdot \vec{v}_2) \left(\vec{S}_1 \times \vec{r} \right)^j \right. \\
&\quad \left. + 6r^i \left(\vec{S}_1 \times \vec{v}_2 \right) + v_2^i \left(\vec{S}_1 \times \vec{r} \right)^j \right\} R_{0i0j},
\end{aligned} \tag{C6}$$

[1] B. P. Abbott et al. GWTC-1: A Gravitational-Wave Transient Catalog of Compact Binary Mergers Observed by LIGO and Virgo during the First and Second Observing Runs. *Phys. Rev.*, X9(3):031040, 2019.

[2]

[3] J. Aasi et al. Advanced LIGO. *Class. Quant. Grav.*, 32:074001, 2015.

[4] F. Acernese et al. Advanced Virgo: a second-generation interferometric gravitational wave detector. *Class. Quant. Grav.*, 32(2):024001, 2015.

[5] Bruce Allen, Warren G. Anderson, Patrick R. Brady, Duncan A. Brown, and Jolien D.E. Creighton. FINDCHIRP: An Algorithm for detection of gravitational waves from inspiraling compact binaries. *Phys. Rev. D*, 85:122006, 2012.

[6] Solomon Endlich, Victor Gorbenko, Junwu Huang, and Leonardo Senatore. An effective formalism for testing extensions to General Relativity with gravitational waves. *JHEP*, 09:122, 2017.

[7] Walter D. Goldberger and Ira Z. Rothstein. An Effective field theory of gravity for extended objects. *Phys. Rev. D*, 73:104029, 2006.

- [8] Rafael A. Porto and Ira Z. Rothstein. The Hyperfine Einstein-Infeld-Hoffmann potential. *Phys. Rev. Lett.*, 97:021101, 2006.
- [9] Rafael A. Porto. The effective field theorist's approach to gravitational dynamics. *Phys. Rept.*, 633:1–104, 2016.
- [10] Michele Levi and Jan Steinhoff. Spinning gravitating objects in the effective field theory in the post-Newtonian scheme. *JHEP*, 09:219, 2015.
- [11] Xian O. Camanho, Jose D. Edelstein, Juan Maldacena, and Alexander Zhiboedov. Causality Constraints on Corrections to the Graviton Three-Point Coupling. *JHEP*, 02:020, 2016.
- [12] Barak Kol and Michael Smolkin. Non-Relativistic Gravitation: From Newton to Einstein and Back. *Class. Quant. Grav.*, 25:145011, 2008.
- [13] Stefano Foffa and Riccardo Sturani. Effective field theory calculation of conservative binary dynamics at third post-Newtonian order. *Phys. Rev. D*, 84:044031, 2011.
- [14] Stefano Foffa and Riccardo Sturani. Dynamics of the gravitational two-body problem at fourth post-Newtonian order and at quadratic order in the Newton constant. *Phys. Rev. D*, 87(6):064011, 2013.
- [15] K. S. Thorne. Multipole Expansions of Gravitational Radiation. *Rev. Mod. Phys.*, 52:299–339, 1980.
- [16] Andrew J. Hanson and T. Regge. The Relativistic Spherical Top. *Annals Phys.*, 87:498, 1974.
- [17] Rafael A. Porto. Post-Newtonian corrections to the motion of spinning bodies in NRGR. *Phys. Rev. D*, 73:104031, 2006.
- [18] Myron Mathisson. Neue mechanik materieller systemes. *Acta Phys. Polon.*, 6:163–2900, 1937.
- [19] Achille Papapetrou. Spinning test particles in general relativity. 1. *Proc. Roy. Soc. Lond. A*, A209:248–258, 1951.
- [20] W.G. Dixon. Dynamics of extended bodies in general relativity. I. Momentum and angular momentum. *Proc. Roy. Soc. Lond. A*, A314:499–527, 1970.
- [21] H. Goldstein. *Classical Mechanics*. Addison-Wesley, 2002.
- [22] B.M. Barker and R.F. O'Connell. Gravitational Two-Body Problem with Arbitrary Masses, Spins, and Quadrupole Moments. *Phys. Rev. D*, 12:329–335, 1975.
- [23] Stefano Foffa and Riccardo Sturani. Effective field theory methods to model compact binaries. *Class. Quant. Grav.*, 31(4):043001, 2014.
- [24] B.M. Barker and R.F. O'Connell. Derivation of the equations of motion of a gyroscope from

the quantum theory of gravitation. *Phys. Rev. D*, 2:1428–1435, 1970.

[25] Kip S. Thorne and James B. Hartle. Laws of motion and precession for black holes and other bodies. *Phys. Rev. D*, 31:1815–1837, 1984.

[26] Eric Poisson and Misao Sasaki. Gravitational radiation from a particle in circular orbit around a black hole. 5: Black hole absorption and tail corrections. *Phys. Rev. D*, 51:5753–5767, 1995.

[27] Lawrence E. Kidder, Clifford M. Will, and Alan G. Wiseman. Spin effects in the inspiral of coalescing compact binaries. *Phys. Rev. D*, 47(10):4183–4187, 1993.

[28] Lawrence E. Kidder. Coalescing binary systems of compact objects to postNewtonian 5/2 order. 5. Spin effects. *Phys. Rev. D*, 52:821–847, 1995.

[29] B.P. Abbott et al. Tests of General Relativity with the Binary Black Hole Signals from the LIGO-Virgo Catalog GWTC-1. *Phys. Rev. D*, 100(10):104036, 2019.

[30] R. Abbott et al. Tests of General Relativity with Binary Black Holes from the second LIGO-Virgo Gravitational-Wave Transient Catalog. 10 2020.

[31] Rene P. Breton, Victoria M. Kaspi, Michael Kramer, Maura A. McLaughlin, Maxim Lyutikov, Scott M. Ransom, Ingrid H. Stairs, Robert D. Ferdman, Fernando Camilo, and Andrea Possenti. Relativistic Spin Precession in the Double Pulsar. *Science*, 321:104–107, 2008.

[32] Benetge Perera et al. The Evolution of PSR J0737-3039B and a Model for Relativistic Spin Precession. *Astrophys. J.*, 721:1193, 2010.

[33] Delphine Perrodin and Alberto Sesana. *Radio pulsars: testing gravity and detecting gravitational waves*, volume 457, pages 95–148. 2018.

[34] Andreas Ross. Multipole expansion at the level of the action. *Phys. Rev. D*, 85:125033, 2012.